International Journal of Nanomedicine

Dovepress
Taylor & Francis Group

Open Access Full Text Article

ORIGINAL RESEARCH

Anti-Arthritis and Biosafety Properties of Green Synthesized Zinc Oxide Nanoparticles Loaded with *Cedrus libani* Extract

Diana Battal Mejjo[1], Ream Nayal[2], Wassim Abdelwahed[3], Mohammad Yaser Abajy[1,4]

[1]Department of Biochemistry and Microbiology, Faculty of Pharmacy, University of Aleppo, Aleppo, Syria; [2]Department of Pharmacognosy, Faculty of Pharmacy, University of Aleppo, Aleppo, Syria; [3]Department of Pharmaceutics and Pharmaceutical Technology, Faculty of Pharmacy, University of Aleppo, Aleppo, Syria; [4]Department of Biochemistry and Microbiology, Faculty of Pharmacy, Arab Private University for Science and Technology, Hama, Syria

Correspondence: Mohammad Yaser Abajy, Email Mohammad.abajy@aust.edu.sy

Purpose: This research was conducted to develop an easy and safe method for synthesizing zinc oxide nanoparticles (ZnO NPs) with the aim of enhancing the efficacy and biosafety of ethanolic *Cedrus libani* (CL) extract and its aqueous fraction (ACL), as a potential preclinical candidate for anti-arthritis applications.

Methods: UV-visible spectrophotometry, Fourier transform infrared spectroscopy, field emission scanning electron microscopy, energy dispersive X-ray spectroscopy analysis, dynamic light scattering, and zeta potential were used to characterize the synthesized ZnO NPs. The optimal synthesis conditions were determined by evaluating the effects of reaction parameters. The anti-arthritis effect was investigated in vitro using albumin denaturation and human red blood cells (HRBCs) membrane stabilization tests. Additionally, Franz cells were used to determine the ex vivo permeability; carrageenan-induced paw edema, C-reactive protein measurement, and erythrocyte sedimentation rate were used to study the in vivo anti-arthritis effect. Biosafety was assessed through acute and subacute dermal toxicity tests.

Results: Both CL and ACL could synthesize ZnO NPs with 71 and 44 nm diameters, respectively. In vitro, synthesized ZnO NPs showed superior anti-arthritis effects compared to sodium diclofenac and plant extracts, with the IC_{50} values for the albumin denaturation test being10.84 and 11.93 µg/mL for CL-ZnO NPs and ACL-ZnO NPs, respectively. The IC_{50} values for the HRBCs membrane stabilization assay were 9.74 and 14.8 µg/mL for CL-ZnO NPs and ACL-ZnO NPs, respectively. The ex vivo permeability study showed high permeability (946.8 µg/h/cm²). In vivo, both synthesized ZnO NPs demonstrated significant inhibition of carrageenan-induced edema, and performed better than sodium diclofenac and plant extracts, with maximum inhibition of 85.96 ±14.21% (CL-ZnO NPs) and 92.97±6.43% (ACL-ZnO NPs). Acute and subacute toxicity evaluations revealed no adverse effects.

Conclusion: The green synthesized ZnO NPs from both CL and ACL had high permeability, superior efficacy, and biosafe which make them a promising natural product for managing arthritis conditions.

Keywords: anti-inflammatory, zinc oxide nanoparticles, Franz cells, human red blood cell membrane stabilization, HRBCs, albumin denaturation, carrageenan-induced rat paw edema, C-reactive protein, CRP, erythrocyte sedimentation rate, ESR, acute dermal toxicity, sub-acute dermal toxicity

Introduction

Inflammation is the physiological reaction of living tissues to the presence of a chemical, biological, or physical agent in the body.[1] An appropriate inflammation response helps to restore tissue structure and function as well as cellular homeostasis.[2] At the molecular level, inflammation is a highly complex process mediated by a complex network of signaling molecules, including cytokines (IL-1β, IL-6, TNF-α), prostaglandins, leukotrienes, nitric oxide, and reactive oxygen species. These mediators contribute to vasodilation, immune cell recruitment, tissue damage, and pain. In chronic

Received: 1 May 2025
Accepted: 4 September 2025
Published: 19 September 2025

© 2025 Mejjo et al. This work is published and licensed by Dove Medical Press Limited. The full terms of this license are available at https://www.dovepress.com/terms.php and incorporate the Creative Commons Attribution – Non Commercial (unported, v4.0) License (http://creativecommons.org/licenses/by-nc/4.0/). By accessing the work you hereby accept the Terms. Non-commercial uses of the work are permitted without any further permission from Dove Medical Press Limited, provided the work is properly attributed. For permission for commercial use of this work, please see paragraphs 4.2 and 5 of our Terms (https://www.dovepress.com/terms.php).

Graphical Abstract

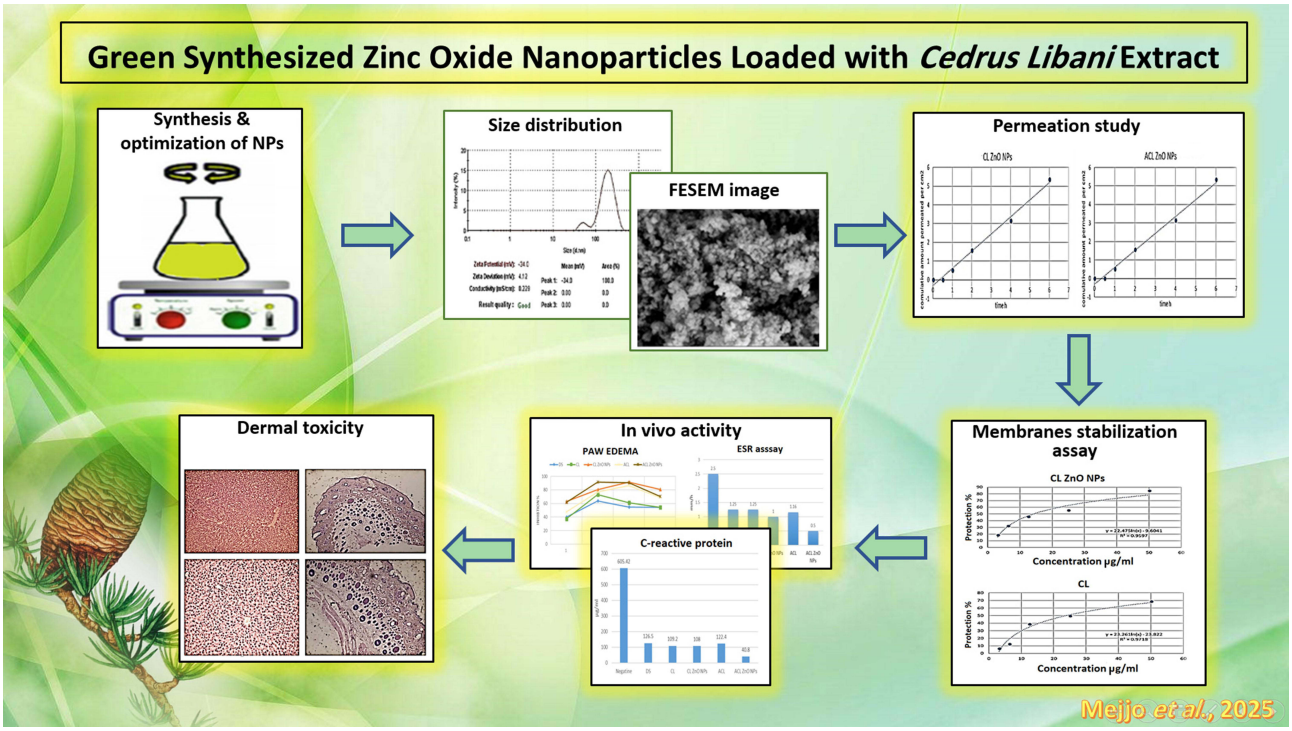

inflammatory diseases such as rheumatoid arthritis, these signaling pathways become dysregulated, leading to progressive tissue destruction and systemic complications.[2,3]

According to the effectiveness of removing the foreign agent or injured tissues,[4] there are primarily two types of inflammation: acute and chronic.[5] Many chronic diseases like rheumatoid arthritis are pathophysiologically linked to prolonged inflammation.[4] According to the World Health Organization (WHO), rheumatoid arthritis (RA) affects 0.3% to 2% of people worldwide, with an increase of 113% since 1990, and women are three times more likely to get it than men.[6]

Non-steroidal anti-inflammatory drugs (NSAIDs) and glucocorticoids are examples of traditional anti-inflammatory medications. Even though NSAIDs are helpful in lowering inflammation, they can lead to serious adverse effects, particularly in the gastrointestinal (GI) tract, such as small intestine mucosal injury.[7] Other risk factors associated with NSAIDs include genetic variations, elevated blood pressure, edema, hepatic or renal dysfunction, hyperkalemia, accelerated asthma, and an increased risk of bleeding.[8,9] On the other hand, glucocorticoids inhibit leukocyte function and reduce inflammation, but they come with their own set of long-term administration side effects and risks.[10]

It is becoming more and more important to check for and develop alternative anti-inflammatory medications due to the drawbacks and possible risks of these abovementioned traditional medications.[11] Investigating medicinal plants, which have been utilized for a long time in conventional medical systems and have demonstrated promise as effective therapeutic agents, is one intriguing direction. Medicinal plants are becoming increasingly popular, as a considerable portion of the world's population now relies on medicinal plants for their health.[4,12] Due to the presence of secondary metabolites, natural plant compounds with anti-inflammatory qualities have been found in several investigations.[13] Due to the phytochemicals obtained from plants' extensive distribution, chemical variety, known biological potentials, and safe toxicological profiles when compared to allopathic medications, the search for effective anti-inflammatory pharmaceuticals from traditional herbal medicine is gaining interest.[14,15]

One of these medicinal plants is *Cedrus libani* (CL), which has been used in ethnomedicine in Lebanon, Syria, and Turkey to cure or control a broad spectrum of illnesses in humans.[16] CL is a 1500–1800 m-high mountain evergreen conifer tree. Native to Lebanon, western Syria, and the western south of Turkey.[17] In Turkey, CL syrup tar is applied externally to wounds and cuts and is used to treat internal sores such as ulcers. Asthma and other upper respiratory diseases were also treated by CL-tar inhalation. In addition, there were several traditional uses for wood oil, such as curing leprosy and respiratory tract diseases. Additionally, toothaches were managed using CL.[16] The effect of using CL and CL extract fraction for the treatment of inflammatory conditions has been proved in previous studies.[18,19]

Plant raw extracts have encouraging biological properties, but they still have a number of issues that need to be solved before they can be used in clinical applications. These issues include poor stability, poor solubility, low absorption, short biological half-life, and quick elimination.[20] Even though phytochemicals have the potential to be bioactive, questions concerning their efficacy, safety, and quality still exist.[21] To increase the phytochemicals' bioavailability for therapeutic usage, recent research has concentrated on creating formulations for plant delivery systems that not only safely carry plant extracts but also increase their therapeutic efficiency.[22] In this regard nanotechnology has emerged as a promising tool to overcome these limitations.[23]

Green nanotechnology represents one of the most favored methods for the production of nanoparticles and contributes to an important symbiosis between phytomedicines and nanotechnology.[23] Its eco-safety, cost-effectiveness, energy-efficiency, and easy large-scale manufacturing of nanomaterials make it a practical technology for synthesizing variously sized and shaped nanoparticles.[24] There are many benefits for phytomedicines in using nanoscale drug delivery methods, such as improving absorption, regulating sustained release, minimizing adverse effects, and masking unpleasant tastes or odors; they also improve solubility, permeability, and stability. These benefits raise the general efficacy, safety, and acceptance of phytomedicines in clinical practice.[25] Specifically in inflammatory diseases, nanoparticle-based formulations can enhance the delivery of phytochemicals to inflamed tissues, provide sustained therapeutic action, and reduce systemic side effects through targeted topical application.[26]

Zinc oxide is an inorganic crystalline semiconductor that is relatively cheap. Compared to other metal and metal oxide nanoparticles, zinc oxide nanoparticles (ZnO NPs) have received a lot of attention because of their exceptional biomedical characteristics, biosafety, and biocompatibility.[23] The FDA has declared ZnO NPs to be a generally recognized as safe (GRAS) substance.[27] ZnO NPs have excellent antibacterial, anti-inflammatory, and wound-healing capabilities.[28] ZnO NPs showed better anti-inflammatory activity compared with other metallic nanoparticles. The ZnO NPs anti-inflammatory mechanism of action goes back to the inhibition of inducible nitric oxide synthase (iNOS) enzyme production, preventing the over-expression of inflammatory responses by inhibiting pro-inflammatory cytokines, suppressing myeloperoxidase, which lowers neutrophil activity, blockage of the NF-κβ pathway, decrease the growth and activation of mast cells, and reducing the expression of the cyclooxygenase 2 (COX-2) gene triggered by LPS. [25]

Previous studies have demonstrated that *Cedrus libani* possesses significant anti-inflammatory activity and that the aqueous fraction of the extract exhibited superior efficacy compared to the ethanolic extract.[18,19] Based on these findings, we conducted this research to develop an easy, cost-effective, and safe method for synthesizing two nano-formulations using CL extracts: CL-ZnO NPs (loaded with the CL ethanolic extract) and ACL-ZnO NPs (loaded with the aqueous fraction), with the aim of enhancing their efficacy, bioavailability, and biosafety and evaluating whether the enhanced bioactivity observed in the aqueous extract is retained or amplified when delivered through zinc oxide nanoparticles. Where no studies have previously been conducted to utilize these extracts for the development of nanostructures and their preparation in forms suitable for clinical anti-arthritis application.

Materials and Methods

Materials

Chemicals used in this study are Butanol (SCP, United Kingdom), Carrageenan, Chloroform (Eurolab, United Kingdom), C-reactive protein latex kit (AMSbio, United Kingdom), Ethanol (Schalau SL, Spain), Ethyl acetate (Sham lab/Fischer, Syria), Diclofenac diethylamine emulgel 1.16% (Vollgel med, MPI Syria), Double-distilled water, Formaldehyde (Merck, Germany), Hexane (SCP, United Kingdom), Normal salin (M&G, Syria), Ketamine

(Sigma-tec, Egypt), Sodium chloride (HiMedia Labs, India), Sodium diclofenac (Amoli Organics Pvt., India), sodium hydroxide (HiMedia Labs, India), Sodium phosphate dibasic dehydrate (sigma Aldrich, Germany), Sodium phosphate monobasic dehydrate (Acros organics, United States), and zinc acetate dihydrate (HiMedia Labs, India). The equipment's utilized are atomic absorption spectrometry (Phoenix-986, United Kingdom), Digital Caliper (Gilbert, China), Electronic balance (Sartoruis AG, Germany), Field emission scanning electron microscopy (Zeiss, Germany), franz cells (SES GmbHA Analysesysteme, Germany), hotplate magnetic stirrer (snijders, Netherlands), refrigerated tabletop centrifuge (Hitachi, Japan), Fourier transform infrared spectroscopy (Bruker, Germany), rotary evaporator (Heidolph Instruments, Germany), Ultra sonic (Hawashin, Korea), UV-1800 spectrophotometer (shimadzu, Japan), V-650 UV spectrophotometer (JASSCO, Japan), water bath (J.P. Selecta, Spain), and Zetasizer (Malvern Panalytical, United Kingdom).

Plant Collection and Identification

Leaves of *Cedrus libani* were gathered from trees on the campus of the University of Aleppo. Botanical identification was performed by Dr. Ahmad Jaddouh of the Faculty of Agriculture. After being cleaned with distilled water and allowed to dry in the shade for three days, the leaves were ground and stored in airtight container away from light, heat, and moisture. A voucher specimen with the number CLL-V36 was deposited in the pharmacognosy and phytochemistry department, faculty of pharmacy, Aleppo university, Syria.

Preparation of Extracts

The ethanolic leaf extract was prepared by macerating 30 g of the leaves in 100 mL ethanol 70% with continuous stirring at room temperature for 24 hours, and the leaves were re-extracted according to the previous method for three times. The dry extract (CL) was obtained by using a rotary evaporator set at 40°C. It was then kept in sealed containers at −10°C. The CL aqueous (ACL) fraction, which has already demonstrated the best anti-inflammatory efficacy among the other fractions, was also prepared.[19] To do this, 2 g of the ethanolic extract were weighed, suspended in 100 mL of distilled water, and extracted using various polar solvents, including hexane, chloroform, ethyl acetate, butanol, and distilled water, respectively. The aqueous fraction was then collected, dried at 40 °C using a rotary evaporator, and kept until needed. [17,29]

Green Synthesis of ZnO NPs

Zinc oxide nanoparticles were synthesized utilizing CL and ACL extracts. To determine the optimal conditions for the synthesis reaction, the effects of the following parameters were examined one by one: the temperature, pH, extracts-to-zinc-acetate-dihydrate ratio, the concentration of zinc acetate dihydrate, and reaction time. And the final optimized synthesize method was as follows: adding CL ethanolic extract 2% solution that prepared freshly from the dried CL extract previously mentioned dropwise to a zinc acetate dihydrate solution at a 4/40 ratio with continued stirring. After ten minutes, a 2 M sodium hydroxide solution was used to adjust the pH to 10. The mixture was then stirred and heated at 60°C for 4 hours, during which the color gradually changed from oily green to brown, indicating zinc oxide precipitation. After centrifuging for five minutes at 10,000 rpm, the precipitate was washed with ethanol and double-distilled water as part of the purification procedure. The brown precipitate was then dried at 60°C for 24 hours, to obtain CL-ZnO NPs. The same steps were used to synthase ACL-ZnO NPs from ACL aqueous extract 2% solution that prepared freshly from the dried ACL extract.

Characterization of ZnO NPs

The synthesized nanoparticles were characterized using UV-visible spectrophotometry, dynamic light scattering (DLS) and zeta potential, Fourier transform infrared spectroscopy (FT-IR), field emission scanning electron microscopy (FESEM), and energy dispersive X-ray spectroscopy analysis (EDX).

UV-Visible Spectrophotometry

Utilized to verify the generation of zinc oxide by measuring the nanoparticle precipitate after it has been resuspended in double-distilled water within the wavelength range of 200 to 800 nm.[30]

Dynamic Light Scattering (DLS) and Zeta Potential

The synthesized ZnO nanoparticle's size was ascertained using DLS after resuspending in double-distilled water. Zeta potential was determined to quantify the charge on the surface and colloidal stability of the biosynthesized ZnO NPs.[31]

Fourier Transform Infrared Spectroscopy (FT-IR)

FT-IR was utilized to verify the incorporation of plant extract into ZnO nanoparticles and to take into account the role that functional groups play in the interactions between biological molecules and metal oxide particles. Using the potassium bromide pellet technique, an FTIR spectrophotometer validated the FTIR spectra at 1 cm^{-1} motion. The frequency array was considered with a wave range of 4500–300 cm^{-1}.[30]

Field Emission Scanning Electron Microscopy (FESEM) and Energy Dispersive X-Ray Spectroscopy Analysis (EDX)

To verify the size, shape, and to identify and quantify the elemental composition of the synthesized ZnO nanoparticle, an FESEM with 5 kV acceleration voltages associated with energy dispersive X-ray spectroscopy was used.[32]

In vitro Anti-Inflammatory Activity

The anti-inflammatory effect of CL-ZnO NPs and ACL-ZnO NPs was tested using human red blood cells (HRBCs) membrane stabilization assay and the albumin denaturation assay.[18,33]

HRBCs Membrane Stabilization Assay

CL-ZnO NPs and ACL-ZnO NPs were evaluated for their protective effects on heat-induced HRBCs hemolysis using a slightly modified version of Shinde et al's methodology.[18]

Preparation of RBCs Suspension

Five milliliters of healthy, non-smoking, non-alcoholic participants' blood were drawn to make the red blood cell suspension. These subjects had not taken any chemical drugs for at least two weeks. The participant's approval was taken before the experiments. After collecting the blood in heparin tubes and centrifuging it for 5 minutes at 3000 rpm, the plasma was removed and replaced with an equal volume of isotonic phosphate buffer (pH 7.4). Following the mixing, the washing procedure was carried out twice. Isotonic phosphate buffer was added after washing to create a 40% red blood cell suspension. The buffer solution is made up of 1 L of distilled water, 1.15 g of NaH_2PO_4, 0.24 g of Na_2HPO_4, and 9 g of NaCl.

Examining the Ability of Synthesized ZnO Nanoparticles to Stabilize RBCs Membranes

A series of dilutions of each plant extract, synthesized ZnO NPs, and sodium diclofenac (DS) as the standard medication were prepared using the phosphate buffer previously indicated. Saline solution was employed as a negative control, and the following concentrations were used: (50, 25, 12.5, 6.25, and 3.125 µg/mL) for plant extracts and ZnO NPs, (100, 50, 25, 12.5, and 6.25 µg/mL) for DS. Each of the two sets of centrifuge tubes held 5 milliliters of test sample, 4.85 milliliters of isotonic buffer solution, and 0.15 milliliters of 40% RBC suspension. One of the groups was placed in a 54 °C water bath for 20 minutes. The other group was placed inside the frigid. Following a 7-minute, 3500 rpm centrifugation of the tubes, the supernatant's absorbance was measured at 560 nm. The ability of the plant extract and synthesized ZnO NPs to stabilize the membrane was determined in percent by the Eq. (1).

$$protection\% = 1 - \left(\frac{A2 - A1}{A3 - A1}\right) \times 100 \quad (1)$$

A1: Absorbance of unheated test sample.

A2: Absorbance of heated test sample.

A3: Absorbance of heated negative control sample.

Determination of Albumin Denaturation

The effects of plant extracts, ACL-ZnO NPs and CL-ZnO NPs on albumin denaturation were assessed utilizing a slightly modified version of the methodology used by Kumari et al.[33]

A reaction mixture containing 0.2 mL of fresh egg white's albumin, 2.8 mL of isotonic phosphate buffer (pH 7.4), and 2 mL of the samples at the following concentrations were prepared: 150,100, 50, 6.25, 3.125 µg/mL for CL, 50, 25, 12.5, 6.25, 3.125 µg/mL for ACL, 150, 100, 50, 6.25, 3.125 µg/mL for CL-ZnO NPs, 50, 25, 12.5, 6.25, 3.125 µg/mL for ACL-ZnO NPs, and 150 µg/mL for DS as the standard drug. After 20 minutes at 37 °C, the mixture was incubated for 5 minutes at 70 °C. The absorbance was measured at 660 nm following cooling. Eq. (2) was utilized to determine the extract's and the synthesized ZnO NPs percentage capacity to shield proteins from denaturation.

$$protiction\% = 1 - \left(\frac{a1}{a2}\right) \times 100 \tag{2}$$

a1: Studied sample absorbance

a2: Negative control absorbance

Preparation of ZnO NPs Gel

To prepare a gel with a concentration of 1% of CL-ZnO NPs and ACL-ZnO NPs, 1 g of nanoparticles was combined with 67 mL of distilled water and vortexed for 5 minutes. Then 1.5 g of carbopol 934 was added and the mixture was stirred for 2 hours. Next, 30 mL of 70% ethanol and 0.5 mL of triethanolamine were incorporated. For the preparation of 1% plant extract gels, 1.5 g of carbopol 934 was mixed with 67 mL of distilled water and stirred for 2 hours. Subsequently, 30 mL of 70% ethanol, 1 g of plant extract, and 0.5 mL of triethanolamine were added. This gel formula preparation method was previously developed in our laboratory.

Ex vivo Permeability Determination

The percutaneous absorption of the CL-ZnO NPs and ACL-ZnO NPs gels was evaluated using the static Franz diffusion method. With the use of a thermostatic water jacket around the cell, 10 mL of phosphate buffer (pH 7.4) solution was equilibrated at 37 °C to form the receptor compartment. A magnetic stirrer was used to continuously stir the buffer solution inside the diffusion cell. A piece of cellulose filter with pore dimensions 0.45 µm was placed between each compartment, with a mean exposed area of approximately 1.76 cm^2. Within the receptor compartment, 1 mL of the solution was removed to maintain sink condition at certain time intervals (0.5, 1, 2, 4, and 6 hours). Immediately after the sample was removed, the same volume of the buffer solution was added.[34] Atomic absorption spectrometry (AAS) was utilized to determine Zn concentration of the samples at wavelength 239 nm with flame type air-acetylene. The analytical measurements were performed using a standard Zn solution (10 µg/mL) diluted in phosphate buffer.

In vivo Anti-Inflammatory Activity

The anti-inflammatory effect was evaluated by carrageenan-induced rat paw edema, c-reactive protein (CRP) determination, and erythrocyte sedimentation rate (ESR).

Animals Used in Experiments

Female Wistar Albino rats weighing between 100 and 150 g were procured from the Aleppo University Faculty of Pharmacy's animal laboratory. Free access to food and water was granted to them. The temperature ranged from 22 to 25 °C, with a 12-hour light-dark cycle. The Ethics Committee of Aleppo University's Faculty of Pharmacy in Syria accepted the study's protocol (registration number: 20/VII 31.11.2023). All experiments and procedures conducted in this study in accordance with the public health guidelines outlined in the Guide for the Care and Use of Laboratory Animals (2011).

Carrageenan-Induced Rat Paw Edema

The procedure for inducing rat paw edema with carrageenan was followed as previously described.[19,35] The rats had a 12-hour fast with unrestricted access to drinking water. They were divided into six groups, each containing 5 female rats. The initial volume of each rat's right paw was measured before the experiment began. Paw edema was induced by

injecting 100 µL of newly made 1% carrageenan suspension in normal saline into the right paw's ankle joint. An hour before the induction of paw edema, approximately 0.3 g of the gels were topically applied to the right rat's paws.[36] The paw volume was measured every hour for four hours after the carrageenan injection by a digital caliper. The inhibition percentage of paw edema was calculated hourly using the designated Eq. (3).

- Group 1: blank gel was applied (negative control)
- Group 2: diclofenac emulgel 1% as standard was applied (positive control)
- Group 3: CL extract 1% gel was applied
- Group 4: ACL extract 1% gel was applied
- Group 5: CL-ZnO NPs 1% gel was applied
- Group 6: ACL-ZnO NPs 1% gel was applied

$$inhibtion\% = 1 - \left(\frac{vas - vbs}{van - vbn}\right) \times 100 \quad (3)$$

Vas: sample paw volume after injection

Vbs: sample paw volume before injection

Van: negative control paw volume after injection

Vbn: negative control paw volume before injection

C-Reactive Protein (CRP) Determination

Following the administration of carrageenan for four hours, blood was obtained via puncturing the retro-orbital plexus under light anesthesia with ketamine on a dry Eppendorf tube, then serum was separated. By using a latex immuno-turbidimetry kit, the serum levels of CRP were quantitatively measured, and the agglutination was countified by spectrophotometer. Furthermore, in order to ascertain the CRP normal range under our test settings, we measured the CRP of three normal female rats at the same age.[37]

Erythrocyte Sedimentation Rate (ESR)

The ESR was measured using the Westergren method four hours after the carrageenan was administered. Under mild anesthesia, blood samples were obtained by puncturing the retro-orbital plexus into tubes containing trisodium citrate. The erythrocyte settling speed was measured in mm/h while Westergren tubes were positioned vertically for a duration of one hour. The ESR of three normal female rats at the same age was also measured to determine the normal range.[38]

Acute Dermal Toxicity

The OECD Guidelines 402 were followed in the acute dermal toxicity investigation.[39] For the tests, female Wistar albino rats weighing between 100 and 180 g were utilized. The females used were non-pregnant. The animals were split up into four groups; each group consists of five rats:

- Group 1: control group
- Group 2: blank gel
- Group 3: CL-ZnO NPs gel
- Group 4: ACL-ZnO NPs gel

Initially, an electric clipper was used to shave 10% of the rats' body surface area in the dorsal region. The shaved area was then topically treated with gels at a dosage of 2000 mg/kg. After that, the treated skin was wrapped with non-irritating tape and gauze dressing for 24 h. In contrast, the control groups received the same treatment that is, gauze moistened with physiological saline applied to their skin.[39] The animals were watched at 0.5, 2, 4, and 24 h post-application. The dressings were taken off after 24 hours, and the animals were monitored for a period of 14 days. On the day of application and daily thereafter, the animals' weight and total individual feed intake were recorded. The

animals were also watched for alterations in behavioral patterns, clinical symptoms, necropsy findings, and mortality. The outcomes were then compared to those obtained from the blank gel and control groups.

Sub-Acute Dermal Toxicity

The sub-acute dermal toxicity study was conducted in accordance with OECD Guidelines 410.[40] Non-pregnant female Wistar albino rats, weighing between 100 and 180 g were used for the experiment.

As in the acute toxicity trial, the animals were divided into four groups of three rats each. Each animal was kept in its own enclosure. The test animals' fur is removed from their dorsal regions, removing at least 10% of their surface area, just prior to testing. The gels were administered at a dosage of 1000 mg/kg every day for 21 days. Animals were weighed once a week and were watched daily for any indications of toxicity.

After the 21-day study period, all animals were sacrificed, and blood samples were collected individually in tubes for clinical chemistry analysis. Biochemical tests were conducted to assess renal, pancreatic, and liver function, alongside a complete blood count examination. On sacrifice day, a tiny portion of the skin, kidney, and liver were removed and kept in formalin for a subsequent histological analysis.

Statistical Analysis

All experiments were performed in triplicate. Results were presented as mean ± standard devi-ation (SD). Statistical analyses were conducted using IBM SPSS Statistics (Version 24). The suitability of parametric tests was evaluated by assessment of normality (Shapiro–Wilk test) and homogeneity of variance (Levene' s test). For data meeting both assumptions one-way ANOVA followed by Tukey's test was done. For datasets violating homogeneity of variance, Welch's ANOVA with subsequent Games-Howell post-hoc testing was performed. $p<0.05$ was considered satatically significant.

Results

Verification of ZnO NPs Synthesis Visually

The color change after a few minutes of incubation, the solutions of both plant extracts turned from oily green to brown, signifying the formation of ZnO NPs (Figure 1).

Reaction Conditions Optimization Using DLS

In order to investigate their impact on the response (size) for the CL-ZnO NPs study, the following process factors were evaluated: temperature (60–80 °C), pH (6–12), CL extract 2% ratio to zinc acetate dihydrate (1/40, 2/40, 4/40, 8/40, and

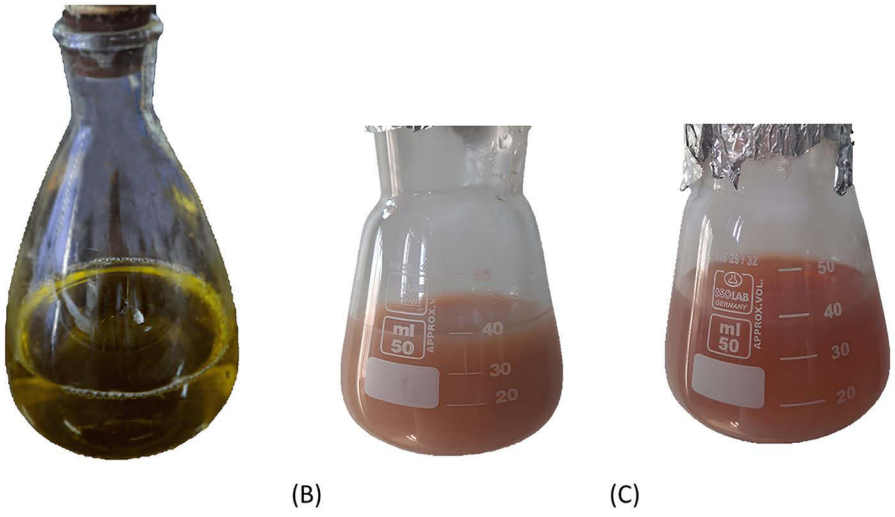

Figure 1 Visual appearance of (**A**) CL ethanolic extract 2% solution (**B**) CL-ZnO NPs and (**C**) ACL-ZnO NPs.

Table 1 The Reaction Parameters for Particle Size Optimization Derived from DLS Analysis

Temperature °C	pH	E/S Ratio	Zn Precursors Concentration M	Time H	Size nm	PDI
25	10	4/40	0.02	2	268.9	0.277
60	10	4/40	0.02	2	164.6	0.259
70	10	4/40	0.02	2	214	0.272
80	10	4/40	0.02	2	190.9	0.167
60	12	4/40	0.02	2	203.6	0.233
60	8	4/40	0.02	2	518.2	0.505
60	6	4/40	0.02	2	1269	0.838
60	10	1/40	0.02	2	438.4	0.322
60	10	2/40	0.02	2	350.9	0.297
60	10	8/40	0.02	2	269.9	0.362
60	10	12/40	0.02	2	658.2	0.300
60	10	4/40	0.01	2	167.9	0.270
60	10	4/40	0.03	2	160	0.239
60	10	4/40	0.02	1	215.2	0.385
60	10	4/40	0.02	4	152.4	0.200
60	10	4/40	0.02	6	169.5	0.346
60	10	4/40	0.02	24	279.5	0.037

Abbreviations: E/S, CL extract/zinc acetate dihydrate; PDI, polydispersity index.

12/40), zinc acetate dihydrate concentration (0.01–0.03 M), and incubation duration (1–24 h) (Table 1). The final optimized conditions found to be temperature 60 °C, pH 10, E/S ratio 4/40, Zn precursors concentration 0.02 M, and reaction time 4 h and after that the final optimized conditions were used to ACL-ZnO NPs synthesis.

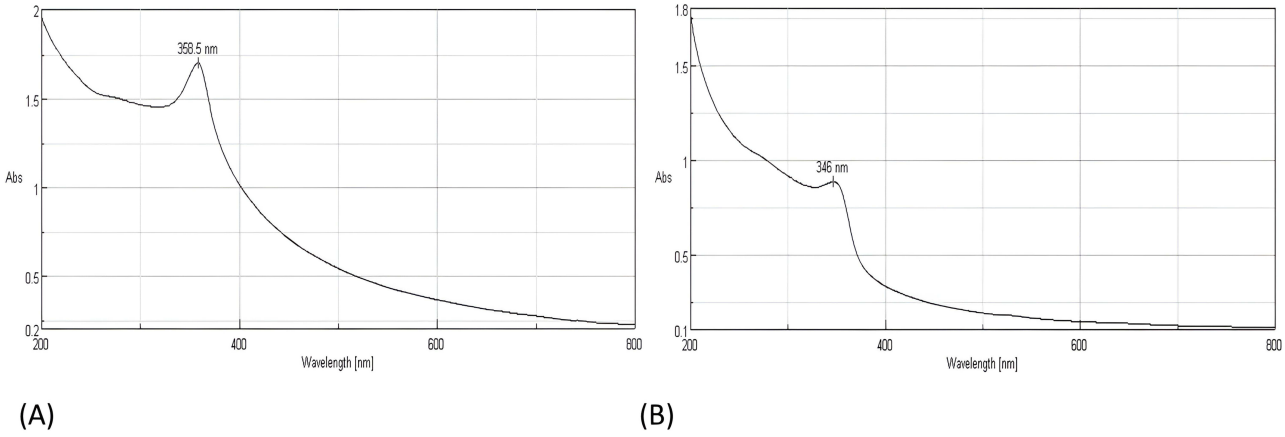

(A) (B)

Figure 2 UV-visible spectra for (**A**) CL-ZnO NPs and (**B**) ACL-ZnO NPs.

https://doi.org/10.2147/IJN.S537934

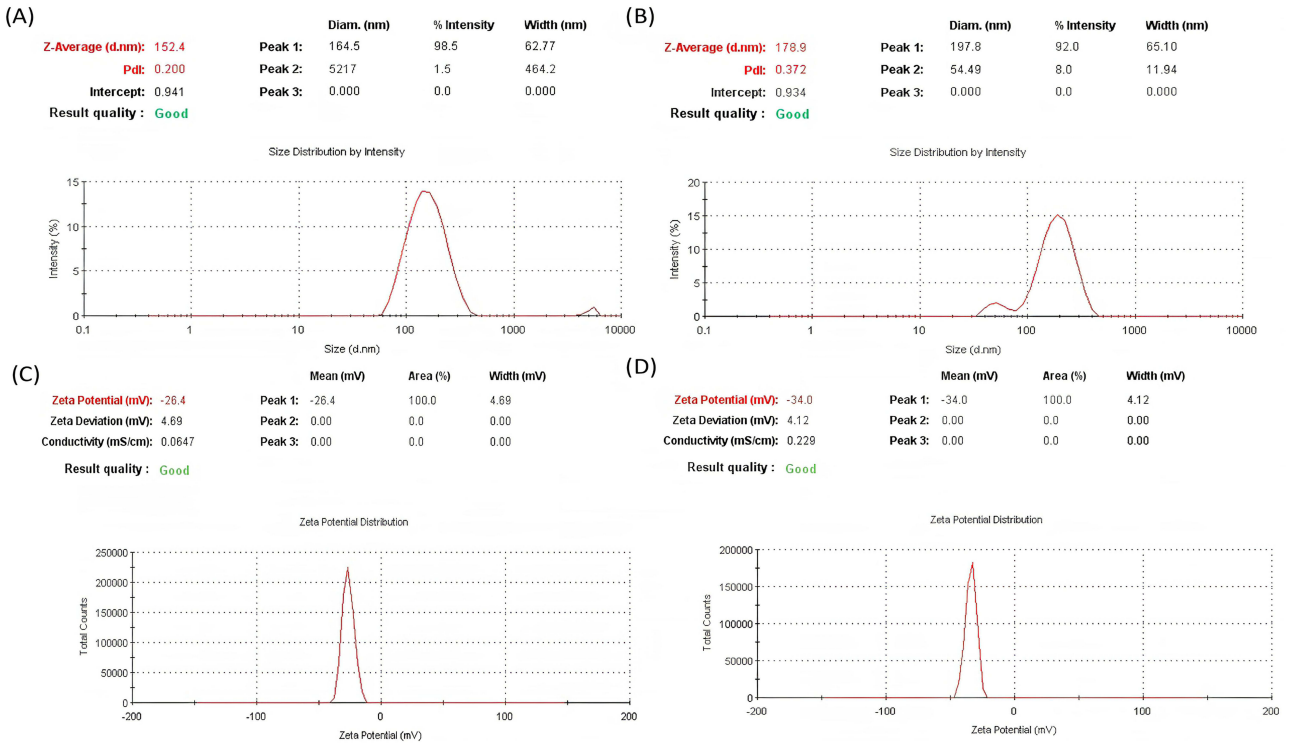

Figure 3 DLS and Zeta potential analyzes (**A**) DLS for CL-ZnO NPs, (**B**) DLS for ACL-ZnO NPs, (**C**) zeta potential for CL-ZnO NPs, (**D**) zeta potential for ACL-ZnO NPs.

Characterization of ZnO NPs

UV-Visible Spectrophotometry

The optimized CL-ZnO NPs and ACL-ZnO NPs' UV-visible analysis is shown in (Figure 2). The spectra of CL-ZnO NPs and ACL-ZnO NPs show the existence of a significant absorption peak at 358.5 nm and 346 nm, respectively.

Dynamic Light Scattering (DLS) and Zeta Potential

The results are displayed in (Figure 3). CL-ZnO NPs and ACL-ZnO NPs had an average particle size of 152.4 nm and 178.9 nm, respectively, and PDI values of 0.200 and 0.372. As seen in (Figure 3), the zeta potential for CL-ZnO NPs and ACL-ZnO NPs was determined to be −26.4 mV and −34 mV, respectively.

Fourier Transform Infrared Spectroscopy (FT-IR)

The produced CL-ZnO NPs and ACL-ZnO NPs' FTIR spectra are displayed in (Figure 4). The (O-H) stretching vibration is represented by the peaks seen at 3234 and 3540 cm-1 for both synthetic ZnO NPs. The (C-H) stretching vibration of aliphatic compounds is responsible for the peaks seen at 2853 and 2924 cm-1 for both synthesized ZnO NPs. The peaks at 1617 and 1638 cm-1 for both produced ZnO NPs are attributable to aromatic (C=O) stretching, while the peaks at 2341 and 2360 cm−1 are associated to the vibration band of alkynes (C=C) stretching. The aromatic CH stretch, the C-OH stretch, and the CH3 bend are represented by the peaks at 1399 in the synthesized ZnO NPs, 1120 and 617 in the CL-ZnO NPs, respectively. CL-ZnO NPs and ACL-ZnO NPs show peaks at 906 and 895 cm-1, respectively, corresponding to Zn-O bending vibrational functional groups, indicating the formation of ZnO particles. The peaks seen at 418 cm-1 in both synthesized ZnO NPs show the distinctive stretching vibration of the Zn-O bond.

Field Emission Scanning Electron Microscopy (FESEM) and Energy Dispersive X-Ray Spectroscopy Analysis (EDX)

The surface morphology of ACL-ZnO NPs and CL-ZnO NPs at several magnifications is depicted in (Figure 5). According to the SEM picture, the majority of the nanoparticles (NPs) in the two produced ZnO NPs have a spherical shape and have diameters of 44 ± 10 nm and 71 ± 22 nm, respectively. As seen in (Figure 5), EDX analysis revealed the

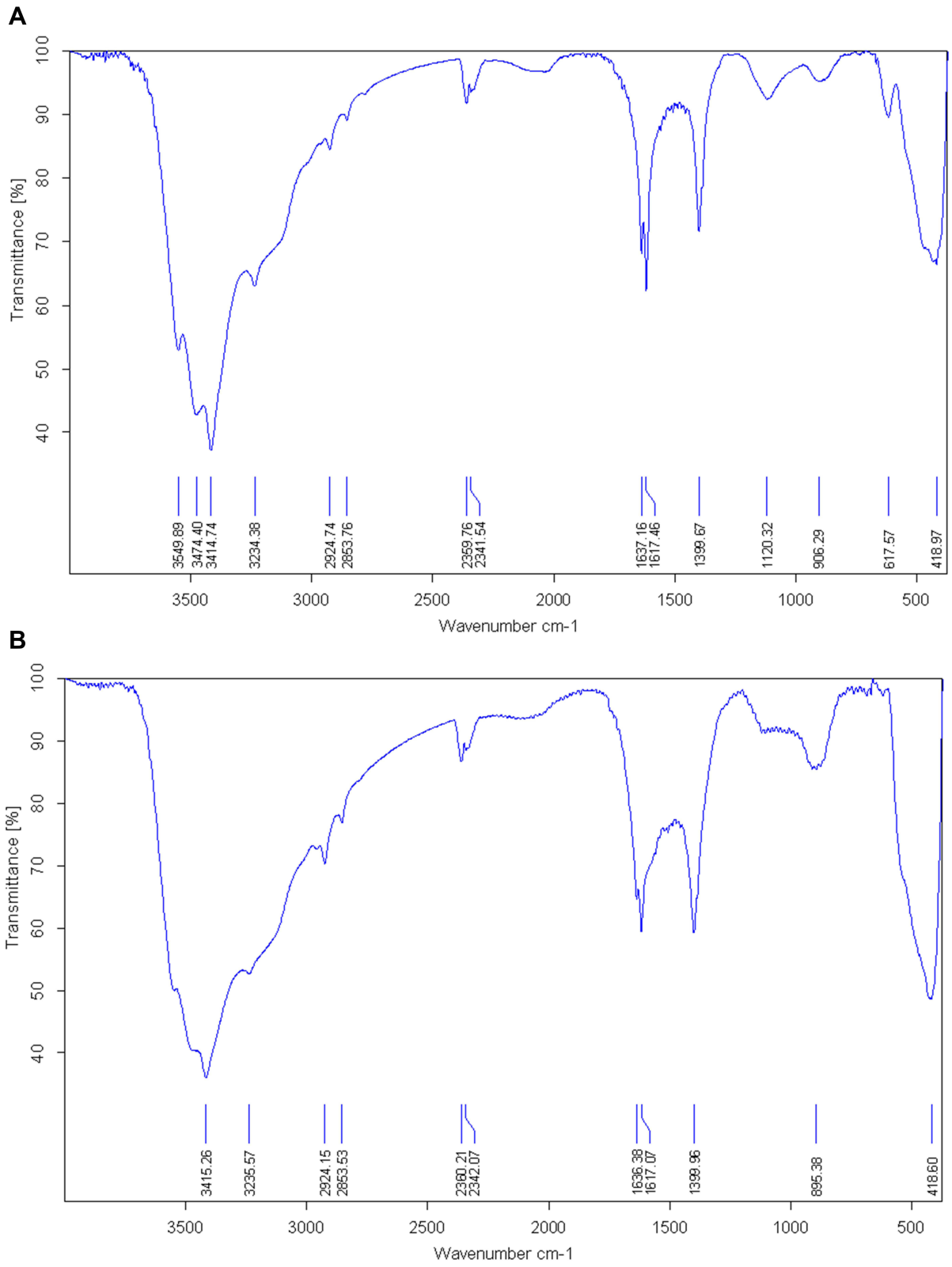

Figure 4 FTIR spectra for (**A**) CL-ZnO NPs and (**B**) ACL-ZnO NPs.

https://doi.org/10.2147/IJN.S537934

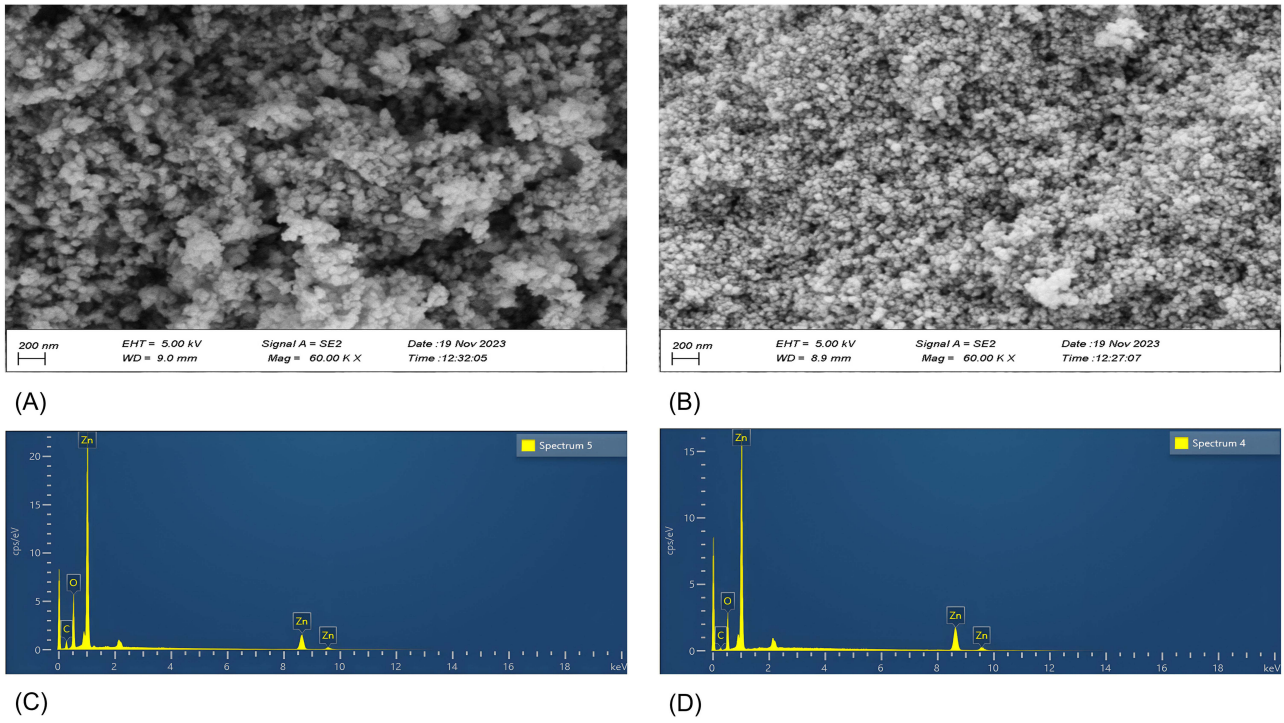

Figure 5 (**A**) FESEM picture of CL-ZnO NPs, (**B**) FESEM picture of ACL-ZnO NPs, (**C**) EDX spectra of CL-ZnO NPs, (**D**) EDX spectra of ACL-ZnO NPs.

peaks that correlated with the existence of oxygen and zinc signals in ZnO NPs. For CL-ZnO NPs and ACL-ZnO NPs, the elemental analysis of the nanoparticle produced 62.63% and 75.15% of zinc and 24.82% and 20.09% of oxygen, respectively.

In vitro Anti-Inflammatory Activity

HRBCs Membrane Stabilization Assay

The findings indicate that plant extract nanoparticles are superior to sodium diclofenac and raw plant extracts in terms of membrane protection, while ACL-ZnO NPs outperform CL-ZnO NPs in terms of protection percentage, with the highest percentages of 91.71% and 84.56% at 50 µg/mL, respectively (Table 2). For ACL-ZnO NPs and CL-ZnO NPs, the IC_{50} was 9.74 and 14.8 µg/mL; for ACL and CL raw extract, it was 10.66 and 23.89 µg/mL; and for DS, it was 37.23 µg/mL (Figure 6). Statistical comparison of the IC_{50} values among the study groups revealed significant differences between all groups, except between CL-ZnO NPs and ACL. All tested samples exhibited significantly lower IC_{50} values compared to DS, with ($p<0.001$) for ACL, ACL-ZnO NPs and ($p<0.01$) for CL and CL-ZnO NPs. The IC_{50} value of CL-ZnO NPs was significantly lower than that of CL raw extract ($p<0.01$), while the IC_{50} value of ACL-ZnO NPs was significantly lower than that of raw ACL extract ($p<0.001$). Furthermore, when comparing the two nanoparticle formulations, ACL-ZnO NPs showed a significantly lower IC_{50} value than CL-ZnO NPs ($p<0.05$).

Determination of Albumin Denaturation

The synthesized nanoparticles showed inhibitory activity against heat-induced albumin denaturation for both extracts (Table 3). The efficacy of the nanoparticles was significantly higher than that of the raw plant extracts at the low concentrations, with IC_{50} values of 10.84 and 11.93 µg/mL for CL-ZnO NPs and ACL-ZnO NPs, respectively. In contrast, the IC_{50} values for the raw plant extracts were 13.88 and 13.72 µg/mL, respectively (Figure 7). Statistical analysis of the IC_{50} values revealed significant differences among all tested groups, except between the CL and ACL extracts, where no significant difference was detected. Both CL-ZnO NPs and ACL-ZnO NPs exhibited markedly lower IC_{50} values compared to both free extracts ($p<0.001$). In addition, the IC_{50} value of CL-ZnO NPs was significantly lower than that of ACL-ZnO NPs ($p<0.05$).

Table 2 The Effectiveness of Zinc Oxide Nanoparticles Loaded with Cedrus libani Extracts on Heat-Induced Hemolysis of HRBCs

Treatment	Concentration µg/mL	Protection % (Mean ± SD)
CL	50	68.38 ± 0.66*
	25	49.25 ± 0.35*
	12.5	38.55 ± 2.06*
	6.25	12.13 ± 1.34*
	3.125	6.32 ± 0.83
CL-ZnO NPs	50	84.56 ± 1.08*#
	25	55.33 ± 2.07*#
	12.5	45.6 ± 1.6*#
	6.25	31.94 ± 1.13*#
	3.125	18.36 ± 1.21#
ACL	50	83.98 ± 1.01*
	25	78.23 ± 1.42*
	12.5	54.07 ± 0.7*
	6.25	37.62 ± 1.54*
	3.125	16.25 ± 0.88
ACL-ZnO NPs	50	91.71 ± 0.74*#+&
	25	79.97 ± 0.87*+
	12.5	57.9 ± 0.7*#+
	6.25	39.53 ± 0.75*+
	3.125	15.51 ± 0.8
DS	100	83.61 ± 0.42
	50	50.74 ± 0.6
	25	44.13 ± 1.25
	12.5	10.68 ± 1.21
	6.25	2.92 ± 0.99

Notes: * $p<0.05$ as compared to DS at the same concentration, # $p<0.05$ as nanoparticles compared to raw plant extract, + $p<0.05$ as ACL-ZnO NPs compered to CL-ZnO NPs, & $p<0.05$ compared to DS 100 µg/mL.

Ex vivo Permeability Determination

The results showed that the skin permeation rate at the steady-state (Jss) was 946.8 µg/h/cm^2 according to the slope value of the straight-line equation with R^2=0.9953 for the first 6 h for both synthetics ZnO NPs, and the percentage of permeation was 38.8% for CL-ZnO NPs and 46.64% for ACL-ZnO NPs, respectively, (Table 4 and Figure 8).

https://doi.org/10.2147/IJN.S537934

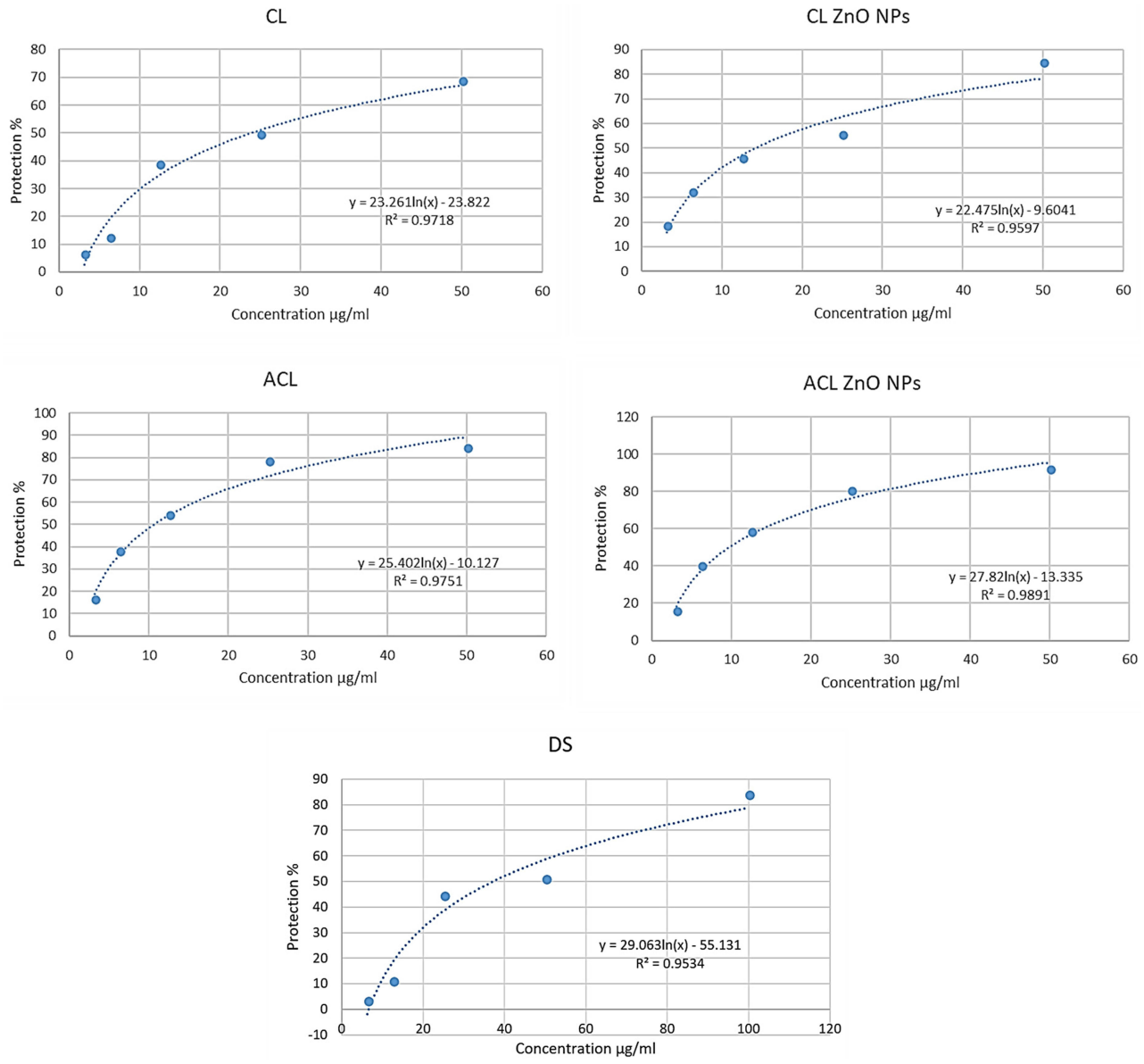

Figure 6 HRBCs membrane stabilization assay IC50 calculation for the synthesized nanoparticles, raw plant extracts, and the positive control.

In vivo Anti-Inflammatory Activity

Carrageenan-Induced Rat Paw Edema

Our study showed that all the synthesized nanoparticles had inhibitory effectiveness against carrageenan-induced edema in rats, as shown in (Table 5 and Figure 9). The effectiveness of the ACL-ZnO NPs was significantly higher than that of DS from the second time interval, while CL-ZnO NPs showed a significant difference compared to DS from the third time interval, where there was a significant difference between the raw plant extract and the nanoparticles only at the third time interval. The nanoparticles reached their highest inhibitory effectiveness at the third interval, with 85.96% and 92.97% for CL-ZnO NPs and ACL-ZnO NPs, while the inhibitory effectiveness was 31.75%, 66.06%, and 86.66% for sodium diclofenac and the raw plant extract, respectively, at the same interval.

The effectiveness of the ACL-ZnO NPs was significantly higher than that of DS from the second time interval ($p<0.05$), while CL-ZnO NPs showed a significant difference compared to DS from the third time interval ($p<0.001$),

Table 3 The Effectiveness of Zinc Oxide Nanoparticles Loaded with Cedrus libani Extracts on Heat-Induced Albumin Denaturation

Treatment	Concentration µg/mL	Inhibition % (Mean ± SD)
CL	150	94.53 ± 0.46*
	100	93.97 ± 1.09*
	50	79.58 ± 0.77*
	6.25	45.25 ± 0.68*
	3.125	7.67 ± 0.47
CL-ZnO NPs	150	96.91 ± 1.04*
	100	94.73 ± 0.59*
	50	82.02 ± 1.23*
	6.25	51.82 ± 1.94*#+
	3.125	14.5 ± 0.86#+
ACL	50	83.66 ± 0.56*
	25	70.18 ± 0.57*
	12.5	45.32 ± 0.53*
	6.25	33.33 ± 0.59
	3.125	4.28 ± 0.71
ACL-ZnO NPs	50	84.53 ± 0.36*
	25	74 ± 0.32*#
	12.5	56.98 ± 0.31*#
	6.25	35.23 ± 0.62
	3.125	5.81 ± 0.71
DS	150	32.36 ± 2.79
	100	–

Notes: * $p<0.05$ as compared to DS, # $p<0.05$ as nanoparticles compared to raw plant extract, + $p<0.05$ as CL-ZnO NPs.

where there was a significant difference between the raw plant extract and the nanoparticles only at the third time interval.

C-Reactive Protein Determination

All the synthesized nanoparticles showed statistically significant effectiveness in reducing CRP values to normal levels compared to the negative Control ($p<0.05$). However, there was no statistically significant difference between the nanoparticles, sodium diclofenac, and the raw plant extracts, as all treatments reduced CRP values to normal levels ($p>0.05$) (Figure 10).

Erythrocyte Sedimentation Rate (ESR)

All the synthesized nanoparticles demonstrated statistically significant efficacy in reducing ESR values compared to the negative control ($p<0.05$) with ACL-ZnO NPs showing enhanced efficacy ($p<0.01$), while neither sodium diclofenac nor

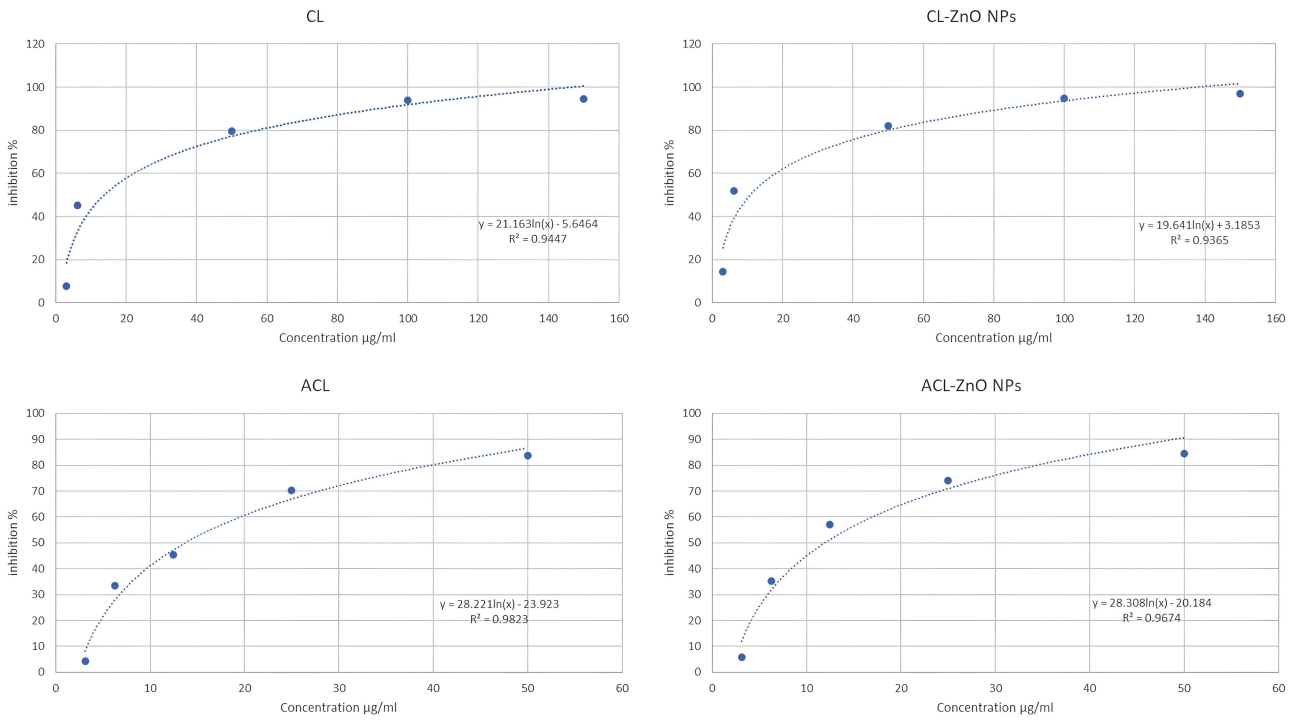

Figure 7 Determination of albumin denaturation IC50 calculation for the synthesized nanoparticles and raw plant extracts.

the raw plant extracts exhibited any statistically significant effectiveness in lowering the ESR values compared to the negative control ($p>0.05$) (Figure 11).

Acute Dermal Toxicity

The studied animals did not show any signs of toxicity, skin irritation, or inflammation during the 14-day study period, and there were no fatalities recorded among the study groups. The results of the study on daily weight changes during the study period did not show any statistically significant difference ($p>0.05$) between the study and the comparison groups (Table 6).

Sub-Acute Dermal Toxicity

No signs of toxicity were observed in the studied animals during the 21-day study period, and no fatalities were recorded. The study of weekly weight changes showed no statistically significant differences ($p>0.05$) between the study groups

Table 4 Ex vivo Permeability Study Results for Synthesized Nanoparticles

Time H	Permeability %	
	ACL-ZnO NPs	CL-ZnO NPs
0.5	2.235	0.745
1	7.835	8.955
2	19.023	18.28
4	38.43	27.98
6	46.64	38.8

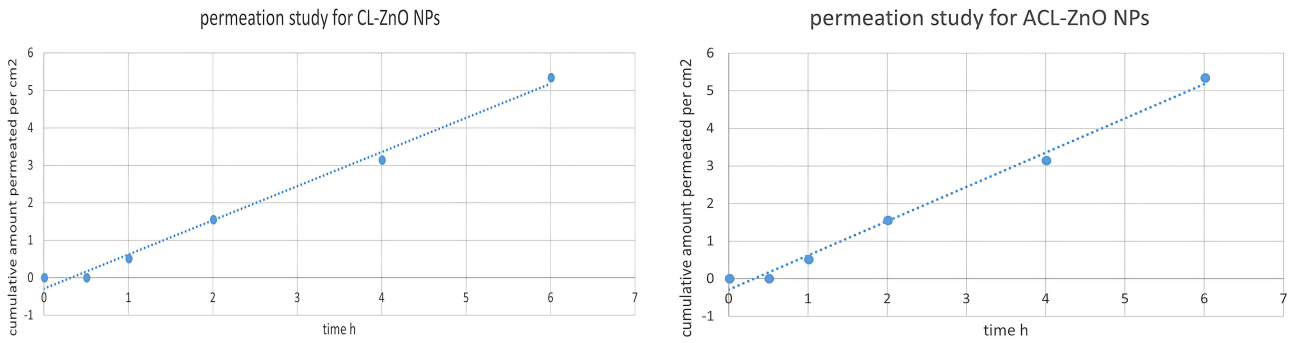

Figure 8 Ex-vivo permeability study results for CL-ZnO NPs and ACL-ZnO NPs.

and the control groups (Table 7). The results of the blood and serum tests showed no statistically significant difference between the values of hemoglobin, red blood cells, white blood cells, platelets, blood sugar levels, liver markers (AST and ALT), and kidney markers (urea and creatinine) between the study groups and the comparison groups (Table 8). The results of the biopsy of the liver, kidneys, and skin were normal in all study groups (Figure 12).

Table 5 The Effectiveness of Synthesized Nanoparticles on the Inhibition of Carrageenan-Induced Edema in Rats

Treatment	Time Hours	Inhibition % (Mean ± SD)
DS	1	52.01 ± 2.76
	2	47.91 ± 17.8
	3	31.75 ± 7.46
	4	31.8 ± 9.54
CL	1	57.28 ± 7.43
	2	85.76 ± 19.49
	3	66.06 ± 14.14*
	4	58.76 ± 6.02
CL-ZnO NPs	1	58.49 ± 9.32
	2	82.63 ± 15.91
	3	85.96 ± 14.21*
	4	76.45 ± 21*
ACL	1	60.8 ± 14
	2	87.84 ± 9.61
	3	86.66 ± 7.89*
	4	61.15 ± 12.21
ACL-ZnO NPs	1	69.22 ± 5.49
	2	92.01 ± 7.39*

(*Continued*)

https://doi.org/10.2147/IJN.S537934

Table 5 (Continued).

Treatment	Time Hours	Inhibition % (Mean ± SD)
	3	92.97 ± 6.43*
	4	76.14 ± 13.57*

Note: * p<0.05 as compared to DS.

Discussion

The color change in the solution was used to visually evaluate the synthesis of CL-ZnO NPs and ACL-ZnO NPs. The solutions of both plant extracts turned from oily green to brown, signifying the formation of ZnO NPs, and a light brown ZnO NPs precipitate was obtained. The observation was consistent with earlier studies on ZnO NPs production that found comparable color changes.[41] DLS technique was used to investigate the impact of temperature, pH, CL extract 2% ratio to zinc acetate dihydrate, zinc acetate dihydrate concentration, and incubation duration on the response size for the CL-ZnO NPs.

In line with earlier research, we found that the reaction pH is the most important parameter in the synthesis of ZnO NPs.[42] With regard to CL extract, we observe that a pH increase led to a decrease in particle size; the ideal size was obtained at a pH of 10. Particle size increased gradually after that when the pH value was raised. This is due to the fact that the pH of the solution affects the electrical charge of molecules, which in turn affects their reduction. An intermediate molecule, such as $Zn(OH)_2$, is seen to develop at higher solution pH levels, allowing for the creation of larger crystallite sizes.[43] The concentration of plant extract was determined to be a second parameter that had an impact on size. Particle size reduced steadily as the concentration of plant extract increased; the ideal size was at a ratio of 4/40; beyond that, concentration increased, causing an increase in particle size. Zinc ions have a tendency to cluster and form bigger particle sizes at lower concentrations of the plant extract due to insufficient capping agent.[44] When extract concentrations are high, there is a greater likelihood of intermolecular interactions and collisions, which in turn causes nanoparticle aggregation.[45] Temperature was the other crucial parameter. When the reaction temperature was increased to 60°C, the particle size decreased; however, further temperature increases led to larger particles. These may result from an elevation in temperature that increases kinetic energy and reaction rate and causes a decrease in particle size. However, excessively high temperatures may inactivate or reduce the activity of the reductive molecules involved in the synthesis,

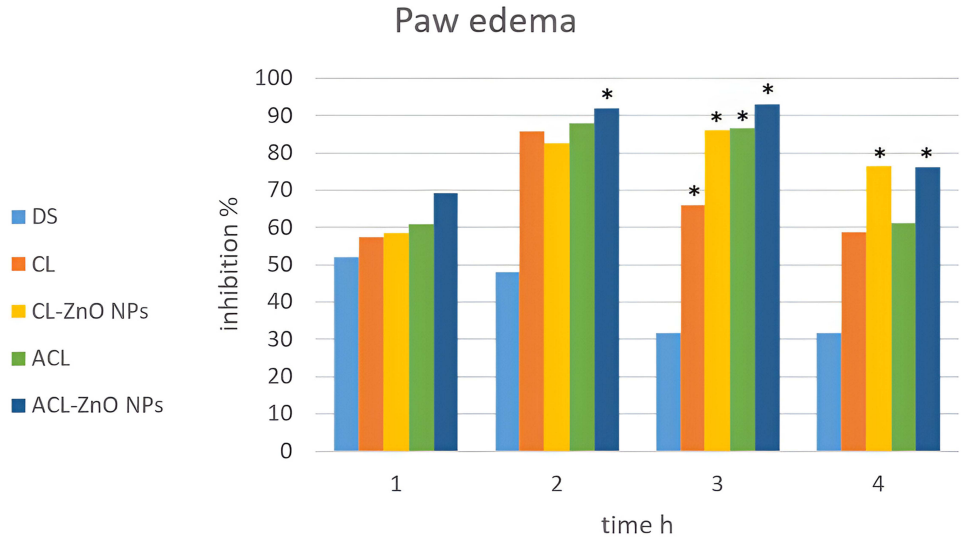

Figure 9 Inhibition of carrageenan-induced rats paw edema for the synthesized nanoparticles (CL-ZnO NPs, ACL-ZnO NPs), raw plant extracts (CL, ACL), and sodium diclofenac (DS). * p<0.05 as compared to DS.

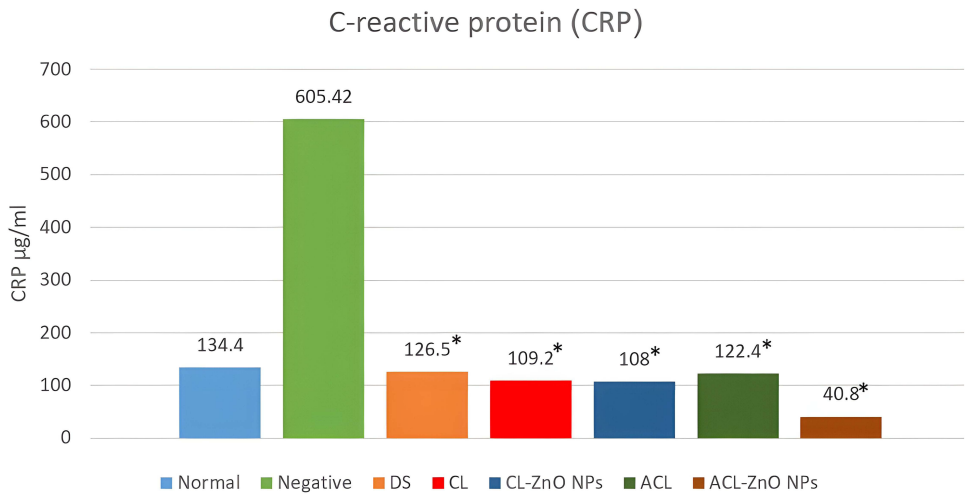

Figure 10 C-reactive protein levels for the synthesized nanoparticles (CL-ZnO NPs, ACL-ZnO NPs), raw plant extracts (CL, ACL), sodium diclofenac (DS), negative control, and normal control. * p<0.05 as compared to negative control.

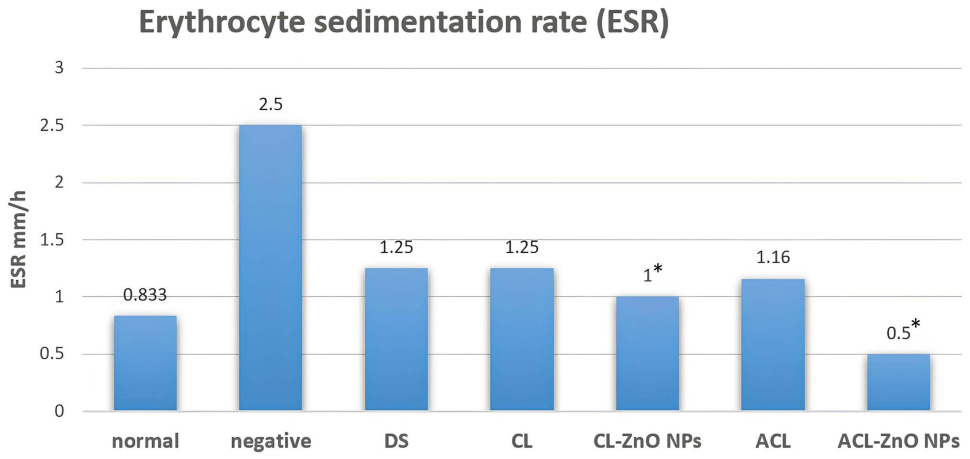

Figure 11 Erythrocyte sedimentation rate for the synthesized nanoparticles (CL-ZnO NPs, ACL-ZnO NPs), raw plant extracts (CL, ACL), sodium diclofenac (DS), negative control, and normal control. * p<0.05 as compared to negative control.

leading to an increase in particle size.[46,47] The optimal duration for the reaction was found to be 4 hours, and a long reaction time was found to increase the size, most likely due to increasing grain growth and collisions between particles that cause aggregation. The effect of reaction time on size appears to be proportionate.[48] The concentration of zinc acetate dihydrate, however, had a minor impact on the size of the particles.

Table 6 Results of Body Weight Changes in the Acute Dermal Toxicity Test

Treatment	Body Weight Changes (g) #		
	Day 1	Day 7	Day 14
CL-ZnO NPs	127.418 ± 6.94	142.19 ± 10.74	149.774 ± 12.75
ACL-ZnO NPs	131.302 ± 32.68	142.796 ± 25.05	151.854 ± 22.52
Blank gel	151 ± 8.74	158.358 ± 7.11	166.17 ± 5.10
Negative control	150.016 ± 21.73	156.298 ± 17.31	166.9 ± 13.39

Note: # (Mean ± SD).

https://doi.org/10.2147/IJN.S537934

Table 7 Body Weight Changes Results in Sub-Acute Dermal Toxicity Test

Treatment	Body Weight Changes (g) #			
	Week 1	Week 2	Week 3	Week 4
CL-ZnO NPs	137.16 ± 5.84	136.88 ± 3.59	146.16 ± 15.91	144.43 ± 2.25
ACL-ZnO NPs	132.81 ± 6.14	138.74 ± 11.2	143.33 ± 9.03	141.72 ± 1.03
Blank gel	172.16 ± 12.88	180.22 ± 12.92	181.98 ± 14.85	188.44 ± 14.69
Negative control	153.99 ±19.08	158.63 ± 18.98	162.19 ± 21.83	162.84 ± 22.57

Note: # (Mean ± SD).

Table 8 Hematology and Biochemistry Results in Sub-Acute Dermal Toxicity Test

Treatment	Hematology (Mean ± SD)				Biochemistry (Mean ± SD)				
	Platelets 10^3/µL	Hemoglobin g/dl	Erythrocytes 10^6/µL	Leucocytes 10^3/µL	ALT U/L	AST U/L	Creatinine mg/dl	Urea mg/dl	Glucose mg/dl
CL-ZnO NPs	906.5 ± 84.14	13.5 ± 0.28	7.185 ± 0.36	3900 ± 1838	53.66 ± 6.65	104.33 ± 15.56	0.493 ± 0.09	30.33 ± 5.68	90.66 ± 26.55
ACL-ZnO NPs	761 ± 2.82	15 ± 0.70	7.45 ± 0.21	6100 ± 2687	41.66 ± 4.04	78 ± 10.14	0.48 ± 0.07	29 ± 4.58	41.33 ± 8.08
Blank gel	814.5 ± 106.7	13.3 ± 0.56	7.51 ± 0.11	5300 ± 848	40.66 ± 14.09	76 ± 23.64	0.54 ± 0.07	32 ± 5.19	78 ± 68.94
Negative control	793 ± 50.86	13.33 ± 0.95	6.95 ± 0.69	4433 ± 1457	47.5 ± 7.77	88.5 ± 12.02	0.43 ± 0.07	24.5 ± 3.53	79 ± 12.72

The UV-visible spectra of CL-ZnO NPs and ACL-ZnO NPs show the existence of a significant absorption peak at 358.5 nm and 346 nm, respectively. This is attributed to ZnO's intrinsic band-gap absorption as a result of electrons moving from the valence band into the conduction band. This phenomenon is known as surface plasmon resonance, and ZnO NPs are known for their propensity to demonstrate it between 310 and 380 nm.[28] The monodispersed character of ZnO NPs is further demonstrated by the strong peaks. The absorption edge progressively moves to a lower wavelength as the nanoparticle's size decreases.[49] This implies that the produced ZnO NPs are small in size, with ACL-ZnO NPs being smaller than CL-ZnO NPs.[50]

The particle size in colloidal solutions can be determined using the commonly used DLS technique. This technique was used to determine the average particle size and PDI of the produced ZnO NPs. CL-ZnO NPs and ACL-ZnO NPs had an average particle size of 152.4 nm and 178.9 nm, respectively, and PDI values of 0.200 and 0.372, indicating that the produced particles are monodispersed.[49,51] In order to know more about the stability of the synthesized ZnO NPs, zeta potential was performed to identify the surface charges of the ZnO NPs. There will not be any NPs aggregation if the particles in a suspension have high negative or positive zeta potential values since they will resist one another. In contrast, there is no force to stop particles from aggregating and coming together if their zeta potential values are low. Zeta potential levels larger than +25 mV or smaller than −25 mV are typically thought to produce stable suspensions.[52] The zeta potential for CL-ZnO NPs and ACL-ZnO NPs was determined to be −26.4 mV and −34 mV, respectively, concluding that ACL-ZnO NPs are more satiable than CL-ZnO NPs because the high negative value supports the particle repulsion and so improves the formulation's stability.

FTIR spectra through unique bond vibration peaks at limited wavenumbers, potential biomolecules that cause ZnO reduction, and capping agents for reduced ZnO NPs were found. Moisture or plant phenolic chemicals may be responsible for the (O-H) stretching vibration peaks. The development of strong aromatic rings and carboxylic acid, which may be in charge of the synthesis of ZnO NPs. The participation of phytochemicals in the reduction and capping of ZnO NPs is

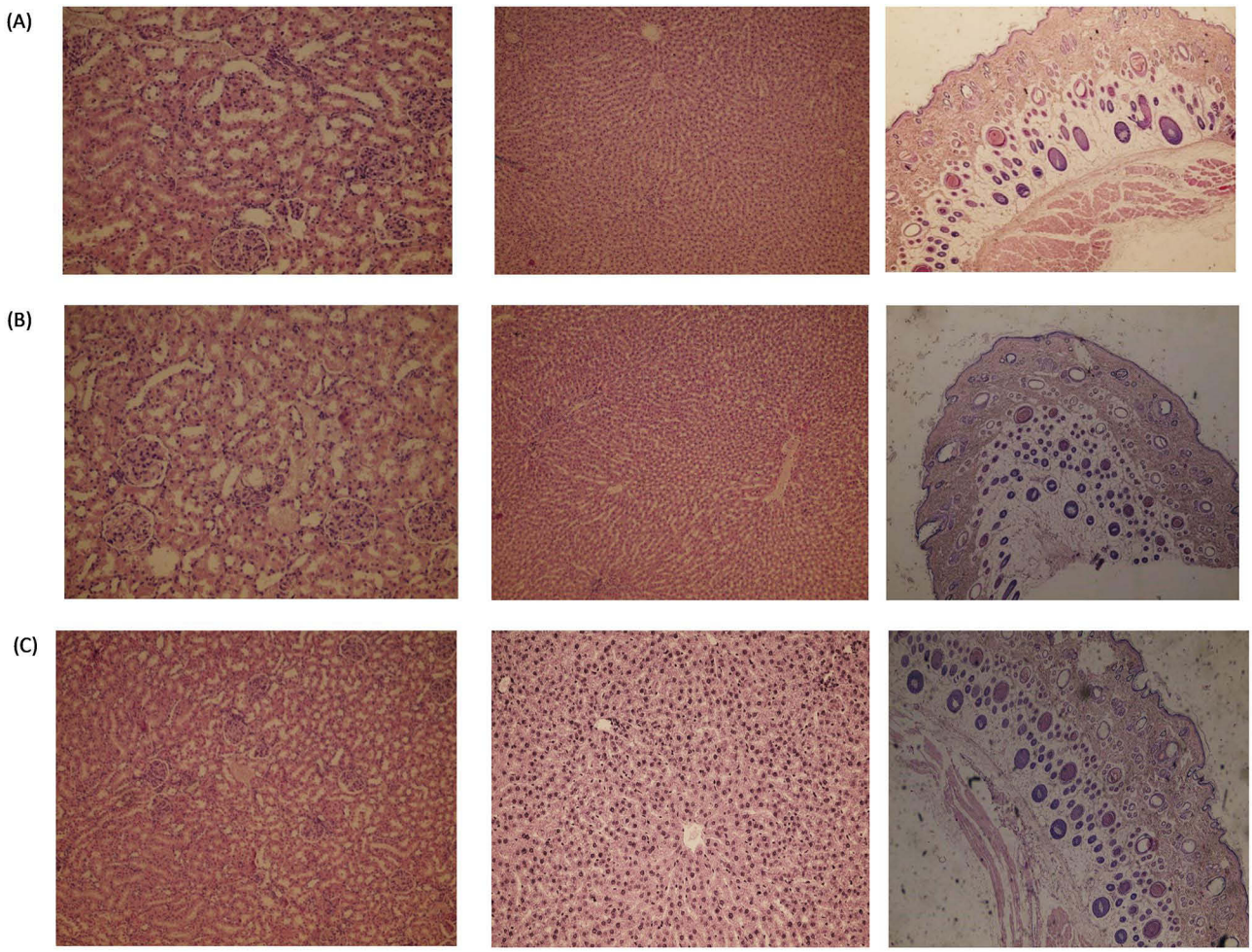

Figure 12 Histology results of kidney, liver and skin from left to right respectively, at magnification of (x40). (**A**) negative control group, (**B**) CL-ZnO NPs group, (**C**) ACL-ZnO NPs group. The histopathology of kidney tissues shows Normal Histopathological appearance of glomeruli surrounded by Bowman's capsule and proximal and distal tubules, the liver tissues show the normal histopathology composed of hexagonal geometric structures containing a central vein and portal spaces, with liver cells arranged in cords separated by sinusoidal vessels. The skin tissues show an absence of any inflammatory signs with a normal appearance of the squamous epithelial cells resting on the basement membrane, and in the dermis, hair follicles, sebaceous glands, and sweat glands are observed.

responsible for the occurrence of C-H stretching vibration and C=C stretching vibration at the surface. CL-ZnO NPs and ACL-ZnO NPs show peaks at 906 and 895 cm^{-1}, respectively, corresponding to Zn-O bending vibrational functional groups, indicating the formation of ZnO particles. The peaks seen at 418 cm^{-1} in both synthesized ZnO NPs show the distinctive stretching vibration of the Zn-O bond. There have been earlier reports of comparable outcomes[53–56]

The size and shape of the produced ZnO NPs were examined using the FESEM. According to the SEM picture, the majority of the nanoparticles (NPs) in the two produced ZnO NPs have a spherical shape and have diameters of 44 ± 10 nm for ACL-ZnO NPs and 71 ± 22 nm for CL-ZnO NPs, respectively. The results of DLS and SEM may differ since they are based on various characterization techniques, and the sample preparation processes are also fundamentally different. This variation is expected, as DLS measures the hydrodynamic diameter of particles in suspension, which includes the solvation layer and possible soft agglomerates, whereas SEM measures the physical diameter of dried individual particles.[57,58] The EDX was studied to estimate the elemental composition of the synthesized ZnO NPs. EDX analysis revealed the peaks that correlated with the existence of oxygen and zinc signals in ZnO NPs it demonstrates that the synthesized nanoparticle is in the purest form possible.[32]

The anti-inflammatory impact was evaluated in vitro using the HRBCs membrane protection approach due to the similarity between HRBCs and lysosomal membranes. By stopping the release of lysosomal contents like proteases,

which causes more tissue damage, stabilization of lysosomal membranes can be essential in reducing inflammatory reactions. Stabilization implies that the green-synthesized ZnO-NPs may successfully stabilize lysosomal membranes.[59] The findings indicate that plant extract nanoparticles are superior to sodium diclofenac and raw plant extracts in terms of membrane protection, while ACL-ZnO NPs outperform CL-ZnO NPs in terms of protection percentage. Our study results are consistent with many previous studies on green synthesized ZnO NPs, where the results showed an effectiveness in protecting the HRBCs membrane comparable to or superior to the protection effect of sodium diclofenac.[60–63] This may be due to the synergistic anti-inflammatory effect between ZnO NPs and the capping phytochemicals, such as polyphenols and flavonoids. CL leaves are abundant in resveratrol, quercetin, and rutin.[16] This phytochemical reduces inflammation by blocking enzymes such as cyclooxygenase, which lowers prostanoids, leukotrienes, and protein kinase C levels. It can also stop mast cells from releasing histamine.[18,59] While ZnO NPs can reduce inflammation in many different ways, like inhibiting (iNOS) enzyme production, pro-inflammatory cytokines, myeloperoxidase, and cyclooxygenase.[25] Previous studies showed that ACL fractions have a higher number of phenols and flavonoids than the ethanolic extract, which may explain the superior activity of ACL ZnO NPs over the CL ZnO NPs.[19]

Protein denaturation is the source of autoantigen formation in inflammation, and multiple studies show that this is one of the causes of inflammation.[64] Researchers discovered that rheumatoid arthritis may be caused by the autoantigen generated by protein denaturation.[65] Due to that agent that has the ability to protect proteins from denaturation, it may have an anti-inflammatory effect. The synthesized nanoparticles showed inhibitory activity against heat-induced albumin denaturation for both extracts. The efficacy of the nanoparticles was significantly higher than that of the raw plant extracts at the low concentrations. Comparing the two synthesized nanoparticles showed that CL-ZnO NPS have a significantly higher effect at the low concentrations. While sodium diclofenac did not show any significant effectiveness at a concentration of 100 µg/mL. Research has shown that green synthesized ZnO NPs are compatible with anti-inflammatory medications, like sodium diclofenac. Compared to sodium diclofenac, ZnO NPs made from an aqueous extract of *Adhatoda vasica* had a greater inhibitory effect on albumin denaturation, according to Dhivyadharshini et al. Meanwhile, Malaiappan et al found that ZnO NPs made from *Catharanthus roseus* extract exhibit an albumin denaturation inhibition effect that is comparable to that of sodium diclofenac. This implies that biosynthesized ZnO NPs are promising anti-inflammatory candidates for application in the future.[66,67]

Given the interest in using the formulation of CL-ZnO NPs and ACL-ZnO NPs for biomedical purposes, primarily topical application, it is necessary to take into consideration the fact that the nanoparticles will release from the gel and permeate through the intact skin. Therefore, an ex vivo permeation study was conducted using the Franz cell method in order to estimate the skin absorption perspective of these nanoparticles. The percentage of permeation was 38.8% for CL-ZnO NPs and 46.64% for ACL-ZnO NPs, respectively. According to the study by Sheferov et al, 58.6% of the synthesized ZnO NPs had permeated after 7 hours of administration. It was clear that Carbopol 934 contributed to regulating the release over an extended duration, and this indicates that sufficient ZnO NPs had penetrated following topical application. This outcome demonstrates that the topical administration of ZnO NPs is a safe and practical candidate for the parenteral route, thereby decreasing the effects of systemic toxicity. As such, it is suitable for the treatment of both acute and chronic local inflammatory reactions.[34,68,69]

This study evaluated the anti-arthritis activity of synthesized CL-ZnO NPS and ACL-ZnO NPs in vivo, selecting 1% gel concentration based on prior studies reporting significant in vivo anti-inflammatory effects at this dose, ensuring consistency and biological relevance.[19] The carrageenan induced paw edema test was performed to assess the anti-inflammatory activity in vivo. Carrageenan injection, which is a seaweed polysaccharide, is a highly sensitive and dependable technique that researchers commonly employ to assess the anti-inflammatory qualities of medications in cases of acute inflammation.[70] Furthermore, it has been shown that the decrease in inflammation brought on by carrageenan is a very reliable indicator of the appropriate dosage for patients.[19] The course of acute inflammation is biphasic. The first phase starts with the release of proinflammatory substances (like histamine, serotonin, and kinins), reactive oxygen, and nitrogen species, which cause edema, hyperalgesia, and erythema in the paw right after subcutaneous delivery. While the second phase is related to the release of prostaglandins and cyclooxygenase in 2–3 hours. According to this hypothesis, the maximum levels of inflammation occur within four hours.[70,71] Our study showed that all the synthesized nanoparticles had inhibitory effectiveness against carrageenan-induced edema in rats. The

effectiveness of the ACL-ZnO NPs was significantly higher than that of DS from the second time interval, while CL-ZnO NPs showed a significant difference compared to DS from the third time interval, where there was a significant difference between the raw plant extract and the nanoparticles only at the third time interval. These findings are in line with prior research showing that green-synthesized ZnO NPs outperform sodium diclofenac and crude extracts. For instance, ZnO NPs derived from *A. citratum* seeds decreased paw edema by 79% after 6 hours of administration, whereas sodium diclofenac only decreased edema by 65% after 3 hours of application, according to Eya'ane Meva et al[72,73] From the above, we can say that the synthesized nanoparticles give a sustained anti-inflammatory effect that may go to the interference of ZnONPs with the release of acute and chronic inflammatory mediators and that the persistent anti-inflammatory activity may be due to the improved permeability and retention effect of zinc oxide nanoparticles in the edema region.[74]

In both acute and chronic inflammatory situations, hepatocytes release C-reactive protein (CRP), an acute phase protein, in response to interleukin-6 (IL-6) and, to a lesser degree, IL-1β and TNF-α. Rats' CRP increased three to four times following an injection of substances that cause inflammation, and it peaked four to twelve hours later.[75–77] All the synthesized nanoparticles showed statistically significant effectiveness in reducing CRP values to normal levels compared to the negative control. These obtained results are consistent with Yadav et al and Jayasri et al, who found a similar CRP reduction after treatment with ZnO NPs. This reduction of acute phase proteins can be attributed to the reduction in the levels of cytokines by nanoparticles.[78,79]

Erythrocyte sedimentation rate (ESR) is an indicator of the erythrocyte's stability in suspension. The ESR is a valuable tool for diagnosing inflammatory diseases, particularly rheumatoid arthritis, and is a crucial indicator for assessing how an animal or a human being reacts to inflammatory and necrotic processes. After the first hour of the carrageenan injection, the ESR peaked because of the high levels of fibrinogen released in the blood during the inflammatory process, which makes red blood cells adhere to one another.[75,80,81] All the synthesized nanoparticles demonstrated statistically significant efficacy in reducing ESR values compared to the negative control, while neither sodium diclofenac nor the raw plant extracts exhibited any statistically significant effectiveness in lowering the ESR values compared to the negative control. An excessive amount of fibrinogen is produced into the blood during the inflammatory process, which makes red blood cells adhere to one another and raises the ESR. According to Kleemann et al, quercetin supplementation significantly decreased the amount of fibrinogen during the atherogenic process. Additionally, Lousinian et al's study showed that fibrinogen adsorption on ZnO NPs results in structural changes that lower fibrinogen activity and ESR levels. It is also known that there is an inverse relationship between aggregate size and specific surface area, meaning that NPs with smaller aggregate sizes have much higher fibrinogen adsorption.[82,83]

The basis for classifying and labeling substances as well as determining their relative toxicity based on the dermal route of exposure is an acute dermal toxicity study. To ascertain whether the synthesized nanoparticles are safe for usage as anti-inflammatory drugs, biological toxicity must be evaluated.[84] The studied animals did not show any signs of toxicity during the 14-day study period, indicating that the toxic dose is higher than 2000 mg/kg.[38] Our results are consistent with the findings of Halarnekar et al, who concluded that the green synthesized ZnO NPs from Nigella sativa are safe for topical use.[85] The toxicity of most nanoparticles increased with concentration and exposure duration. Since nanoparticles can enter the bloodstream and reach fetal organs, prolonged exposure through the skin should be thoroughly investigated for potential clinical anti-inflammatory nanoparticles.[86] No signs of toxicity were observed in the studied animals during the 21-day study period, suggesting that 1% ACL-ZnO NPs and CL-ZnO NPs gels are potentially safe to use.[42] These results are in contrast with Ezealisiji et al's findings, which conclude that green synthesized ZnO NPs from *Solanum torvum* topical chronic application could affect hepatic and renal performance in rats.[87]

Conclusion

The plant extracts of both CL and ACL demonstrated their ability to reduce zinc salts to produce ZnO NPs. The study revealed that the ideal conditions for synthesizing ZnO NPs using CL and ACL extracts were as follows: a temperature of 60°C, a pH of 10, a plant extract to zinc acetate ratio of 4/40, a zinc acetate concentration of 0.02 M, and a reaction time of 4 hours. The study also revealed that temperature and pH were the most influential factors on the quality of the

synthesis, followed by the plant extract to zinc acetate ratio. Meanwhile, changes in time and the concentration of zinc acetate did not have a significant impact on the quality of the synthesis. The study showed that green synthesis of ZnO NPs from CL and ACL extracts gave NPs with dimensions of 71 and 44 nm, respectively, and high stability and purity, according to the results of both zeta potential and EDX.

ACL-ZnO NPs demonstrated greater anti-inflammatory efficacy than CL-ZnO NPs in the albumin denaturation inhibition test, whereas CL-ZnO NPs demonstrated greater anti-inflammatory efficacy than ACL-ZnO NPs in the HRBCs membrane stabilization test, and both ZnO NPs outperformed sodium diclofenac and raw plant extracts. However, the study on the anti-inflammatory efficacy in vivo revealed that the anti-inflammatory activity of nanoparticles was superior to that of both raw plant extracts and sodium diclofenac, as evidenced by the inhibition of carrageenan-induced edema. The highest efficacy was found in ACL-ZnO NPs. Furthermore, the ZnO NPs showed higher effectiveness than both sodium diclofenac and raw plant extracts in reducing ESR values in vivo. In addition, the toxicity studies showed that the synthesized ZnO NPs are non-toxic and biosafe for clinical use. The excellent stability, high permeability, superior efficacy, and biosafety make them a promising natural product for managing inflammatory conditions. Although the in vivo results demonstrated promising anti-inflammatory and biosafety properties, future work should include in vitro cytotoxicity assays to further evaluate the safety profile of the synthesized nanoparticles at the cellular level, and further studies should be performed in order to demonstrate the long-term use toxicity for potential use of ZnO NPs in clinics.

Abbreviations

ZnO NPs, Zinc Oxide Nanoparticles; CL, *Cedrus libani*; ACL, Aqueous *Cedrus libani* Fraction; FT-IR, Fourier Transform Infrared Spectroscopy, FESEM, Field Emission Scanning Electron Microscopy; EDX, Energy Dispersive X-Ray Spectroscopy Analysis; DLS, Dynamic Light Scattering; HRBCs, Human Red Blood Cell; CRP, C-Reactive Protein; ESR, Erythrocyte Sedimentation Rate; IC50, Half Maximal Inhibitory Concentration; CL-ZnO NPs, *Cedrus libani* Zinc Oxide Nanoparticles; ACL-ZnO NPs, Aqueous *Cedrus libani* Fraction Zinc Oxide Nanoparticles; WHO, World Health Organization; NSAIDs, Non-Steroidal Anti-Inflammatory Drugs; GI, Gastrointestinal; FDA, Food And Drug Administration; GRAS, Generally Recognized As Safe; iNOS, Inducible Nitric Oxide Synthase; COX-2, Cyclooxygenase 2; DS, Sodium Diclofenac; AAS, Atomic Absorption Spectrometry; OECD, Organization For Economic Co-Operation and Development; SD, Standard Deviation; E/S, CL Extract/Zinc Acetate Dihydrate; PDI, Polydispersity Index; AST; Aspartate Transferase; ALT, Alanine Transaminase.

Acknowledgment

This research did not receive any specific grant from funding agencies in the public, commercial, or not-for-profit sectors.

Disclosure

The authors report no conflicts of interest in this work.

References

1. Denko CW. A role for neuropeptides in inflammation. In: *Biochemistry of Inflammation*. Dordrecht: Springer Netherlands;1992:177–181. doi:10.1007/978-94-011-2996-1_9
2. Gunalan G, Vijayalakshmi K, Saraswathy A, et al. Anti-inflammatory activities of phytochemicals from Bauhinia variegata Linn. leaf: an in silico approach. *J Chem Pharm*. 2014;6(9):334–48.
3. Libby P. Inflammatory mechanisms: the molecular basis of inflammation and disease. *Nutr Rev*. 2007;65(suppl_3):S140–S146. doi:10.1301/nr.2007.dec.S140-S146
4. Kishore N, Kumar P, Shanker K, et al. Human disorders associated with inflammation and the evolving role of natural products to overcome. *Eur J Med Chem*. 2019;179:272–309. doi:10.1016/j.ejmech.2019.06.034
5. Nagai Y, Honda H, Watanabe Y, et al. Potential therapeutic natural products for the treatment of obesity-associated chronic inflammation by targeting TLRs and inflammasomes. *Chronic Inflamm*. 2016:379–397. doi:10.1007/978-4-431-56068-5_30.
6. GBD. Global burden of 369 diseases and injuries in 204 countries and territories, 1990–2019: a systematic analysis for the global burden of disease study 2019. 2019. Available from: https://vizhub.healthdata.org/gbd-results/. Accessed September 5, 2025.
7. Jiayang L, Kuang Y, Shi J, et al. The conjugation of nonsteroidal anti-inflammatory drugs (NSAID) to small peptides for generating multifunctional supramolecular nanofibers/hydrogels. *Beilstein J Org Chem*. 2013;9(1):908–917. doi:10.3762/bjoc.9.104

8. Sabbagh A, Abajy MY. Investigating the single nucleotide polymorphism A1166C in angiotensin II type 1 receptor gene and its association with hypertension in patients in Syria. *Int J Acad Sci Res*. 2016;4(1):66–75.
9. Kasturi J, Palla PR, Bakshi V, Bogg N. Non-steroidal anti-inflammatory drugs: an overview. *J Drug Delivery Ther*. 2019. doi:10.22270/jddt.v9i1-s.2287
10. Barnes PM, Powell-Griner E, McFann K, Nahin RL. Complementary and alternative medicine use among adults: United States, 2002. In: *Seminars in Integrative Medicine*. WB Saunders; 2004: 2:54–71. doi:10.1016/j.sigm.2004.07.003.
11. Srinivasan K, Muruganandan S, Lal J, et al. Evaluation of anti-inflammatory activity of Pongamia pinnata leaves in rats. *J Ethnopharmacol*. 2001;78(2–3):151–157. doi:10.1016/S0378-8741(01)00333-6
12. Takla S. Investigating in vitro the hemostatic effect of some medicinal plants. *Res J Aleppo Univ*. 2015;100:1–14.
13. Wen D, Liu Y, Li W, et al. Separation methods for antibacterial and antirheumatism agents in plant medicines. *J Chromatogr B*. 2004;812 (1–2):101–117.
14. Mishra BB, Tiwari VK. Natural products: an evolving role in future drug discovery. *Eur J Med Chem*. 2011;46(10):4769–4807. doi:10.1016/j.ejmech.2011.07.057
15. Butler MS, Robertson AAB, Cooper MA. Natural product and natural product derived drugs in clinical trials. *Nat Product Rep*. 2014;31 (11):1612–1661. doi:10.1039/C4NP00064A
16. Ream N, Abajy MY, Bakour AA. Phytochemicals and bioactivities of Cedrus libani A Rich. *Bull Pharmaceut Sci Assiut Univ*. 2023;881–897. doi:10.21608/bfsa.2023.327566
17. Saab AM, Gambari R, Sacchetti G, et al. Phytochemical and pharmacological properties of essential oils from Cedrus species. Nat Product Res. 2018;32(12):1415–1427. doi:10.1080/14786419.2017.1346648
18. Karrat L, Abajy MY, Nayal R. Investigating the anti-inflammatory and analgesic properties of leaves ethanolic extracts of Cedrus libani and Pinus brutia. *Heliyon*. 2022;8(4):e09254. doi:10.1016/j.heliyon.2022.e09254
19. Albakour AA, Nayal R, Abajy MY. Anti-inflammatory and analgesic activity of fractions of Pinus brutia and Cedrus libani leaves ethanolic extracts. *Bull Pharmaceut Sci Assiut Univ*. 2024;47(2):867–882. doi:10.21608/bfsa.2024.279432.2070
20. Neves A R, Lucio M, L.C. Lima J, et al. Resveratrol in medicinal chemistry: a critical review of its pharmacokinetics, drug-delivery, and membrane interactions. *Curr Med Chem*. 2012;19(11):1663–1681. doi:10.2174/092986712799945085
21. Alharbi WS, Almughem FA, Almehmady AM, et al. Phytosomes as an emerging nanotechnology platform for the topical delivery of bioactive phytochemicals. *Pharmaceutics*. 2021;13(9):1475. doi:10.3390/pharmaceutics13091475
22. Husni P, Ramadhania ZM. Plant extract loaded nanoparticles. *Indonesian J Pharmaceut*. 2021;3(1):38–49. doi:10.24198/idjp.v3i1.34032
23. Agarwal H, Shanmugam V. A review on anti-inflammatory activity of green synthesized zinc oxide nanoparticle: mechanism-based approach. *Bioorg Chem*. 2020;94:103423. doi:10.1016/j.bioorg.2019.103423
24. Prasad AR, Williams L, Garvasis J, et al. Applications of phytogenic ZnO nanoparticles: a review on recent advancements. *J Mol Liq*. 2021;331:115805.
25. Nayal R, Mejjo D, Abajy MY. Anti inflammatory properties and safety of green synthesized metal and metal oxidenanoparticles: a review article. *Eur J Med Chem Rep*. 2024;11:100169. doi:10.1016/j.ejmcr.2024.100169
26. Conte R, Marturano V, Peluso G, Calarco A, Cerruti P. Recent advances in nanoparticle-mediated delivery of anti-inflammatory phytocompounds. *Int J Mol Sci*. 2017;18(4):709. doi:10.3390/ijms18040709
27. Bhuyan T, Mishra K, Khanuja M, et al. Biosynthesis of zinc oxide nanoparticles from Azadirachta indica for antibacterial and photocatalytic applications. *Mater Sci Semicond Process*. 2015;32:55–61. doi:10.1016/j.mssp.2014.12.053
28. Yuvakkumar R, Suresh J, Hong SI. Green synthesis of zinc oxide nanoparticles. *Adv Mater Res*. 2014;952:137–140. doi:10.4028/www.scientific.net/AMR.952.137
29. Hossain MA, Al-Hdhrami SS, Weli AM, et al. Isolation, fractionation and identification of chemical constituents from the leaves crude extracts of Mentha piperita L grown in Sultanate of Oman. *Asian Pac J Trop Biomed*. 2014;4:S368–S372. doi:10.12980/APJTB.4.2014C1051
30. Fenglian W, Chen Y, Li G, et al. Zinc oxide nanoparticles synthesized from Allium cepa prevents UVB radiation mediated inflammation in human epidermal keratinocytes (HaCaT cells). *Artif Cells Nanomed Biotechnol*. 2019;47(1):3548–3558. doi:10.1080/21691401.2019.1642905
31. Flemban TH. Synthesis, characterization, and analysis of zinc oxide nanoparticles using varying pulsed laser ablation energies in liquid. *J Exp Nanosci*. 2023;18(1):2175817. doi:10.1080/17458080.2023.2175817
32. Yedurkar S, Maurya C, Mahanwar P. Biosynthesis of zinc oxide nanoparticles using ixora coccinea leaf extract—a green approach. *Open J Synthesis Theory Appl*. 2016;5(1):1–14. doi:10.4236/ojsta.2016.51001
33. Kumari CS, Yasmin N, Hussain MR, Babuselvam M. Invitro anti-inflammatory and anti-artheritic property of Rhizopora mucronata leaves. *Int J Pharm Sci Res*. 2015;6:482–485.
34. Abu-Huwaij R, Abbas MM, Al-Shalabi R, et al. Synthesis of transdermal patches loaded with greenly synthesized zinc oxide nanoparticles and their cytotoxic activity against triple negative breast cancer. *Appl Nanosci*. 2022;12:69–78. doi:10.1007/s13204-021-02166-y
35. Ben Khedir S, Mzid M, Bardaa S, Moalla D, Sahnoun Z, Rebai T. In vivo evaluation of the anti-inflammatory effect of pistacia lentiscus fruit oil and its effects on oxidative stress. *Evidence-Based Complementary Alternative Med*. 2016;2016(1):6108203. doi:10.1155/2016/6108203
36. Pashmforosh M, Rajabi Vardanjani H, Rajabi Vardanjani H, Pashmforosh M, Khodayar MJ. Topical anti-inflammatory and analgesic activities of citrullus colocynthis extract cream in rats. *Medicina*. 2018;54(4):51. doi:10.3390/medicina54040051
37. Yoon JJ, Sohn EJ, Kim JH, et al. Anti-rheumatoid Arthritis Effect of Kaejadan via Analgesic and Antiinflammatory Activity in vivo and in vitro. Phytother Res. 2017;31(31.3):418–424. doi:10.1002/ptr.5763
38. Rahman H, Rahman N, Haris M, Mahmood R. Antioxidant and anti-inflammatory potentials of Solanum pubescens Willd an ethnomedicinal plant of South Western Andhra Pradesh, India. *J Res Pharm*. 2019;(23):187–197. doi:10.12991/jrp.2019.124
39. Mielke H, Strickland J, Jacobs MN, et al. Biometrical evaluation of the performance of the revised OECD Test Guideline 402 for assessing acute dermal toxicity. *Regulatory Toxicol Pharmacol*. 2017;89:26–39. doi:10.1016/j.yrtph.2017.07.007
40. OECD guidelines for testing of chemicals: repeated dose dermal toxicity:21/28-day study. OECD guideline for testing chemicals. 1981;410:1–8.
41. Alrubaie EAA, Kadhim RE. Synthesis of ZnO nanoparticles from olive plant extract. *Plant Archives*. 2019;19(2):339–344.
42. Al-Kordy HMH, Soraya AS, Mabrouk MEM. Statistical optimization of experimental parameters for extracellular synthesis of zinc oxide nanoparticles by a novel haloalaliphilic Alkalibacillus sp. W7. *Sci Rep*. 2021;11(1):10924. doi:10.1038/s41598-021-90408-y

43. Shaba EY, Jacob JO, Tijani JO, et al. A critical review of synthesis parameters affecting the properties of zinc oxide nanoparticle and its application in wastewater treatment. *Appl Water Sci*. 2021;11(2):48. doi:10.1007/s13201-021-01370-z
44. Bakshi MS. How surfactants control crystal growth of nanomaterials. *Cryst Growth Des*. 2016;16(2):1104–1133. doi:10.1021/acs.cgd.5b01465
45. Birla SS, Gaikwad SC, Gade AK, et al. Rapid Synthesis of Silver Nanoparticles from Fusarium oxysporum by Optimizing Physicocultural Conditions. Sci World J. 2013;2013(1):796018. doi:10.1155/2013/796018
46. Husseiny SM, Salah TA, Anter HA. Biosynthesis of size controlled silver nanoparticles by Fusarium oxysporum, their antibacterial and antitumor activities. *Beni-Suef Univ J Basic Appl Sci*. 2015;4(3):225–231. doi:10.1016/j.bjbas.2015.07.004
47. Bandeira M, Giovanela M, Roesch-Ely M, et al. Green synthesis of zinc oxide nanoparticles: a review of the synthesis methodology and mechanism of formation. *Sustainable Chem Pharm*. 2020;15:100223. doi:10.1016/j.scp.2020.100223
48. Gupta A, Srivastava P, Bahadur L, et al. Comparison of physical and electrochemical properties of ZnO prepared via different surfactant-assisted precipitation routes. *Appl Nanosci*. 2015;5(7). doi:10.1007/s13204-014-0379-1
49. Rajakumar G, Thiruvengadam M, Mydhili G, et al. Green approach for synthesis of zinc oxide nanoparticles from Andrographis paniculata leaf extract and evaluation of their antioxidant, anti-diabetic, and anti-inflammatory activities. *Bioprocess Biosyst Eng*. 2018;41:21–30. doi:10.1007/s00449-017-1840-9
50. Tiwari AK, Jha S, Tripathi SK, et al. Antioxidant response of Calendula officinalis L. assisted synthesized zinc oxide nanoparticles. *Mater Res Express*. 2024;11(8):85005. doi:10.1088/2053-1591/ad6ca9
51. Sizochenko N, Mikolajczyk A, Syzochenko M, et al. Zeta potentials (ζ) of metal oxide nanoparticles: a meta-analysis of experimental data and a predictive neural networks modeling. *NanoImpact*. 2021;22:100317. doi:10.1016/j.impact.2021.100317
52. Senthilkumar SR, Sivakumar T. Green tea (Camellia sinensis) mediated synthesis of zinc oxide (ZnO) nanoparticles and studies on their antimicrobial activities. *Int J Pharm Pharm Sci*. 2014;6(6):461–465.
53. Jayappa MD, Ramaiah CK, Kumar MAP, et al. Green synthesis of zinc oxide nanoparticles from the leaf, stem and in vitro grown callus of Mussaenda frondosa L.: characterization and their applications. *Appl Nanosci*. 2020;10(10):3057–3074. doi:10.1007/s13204-020-01382-2
54. Yadav E, Singh D, Yadav P, et al. Comparative evaluation of Prosopis cineraria (L.) druce and its ZnO nanoparticles on scopolamine induced amnesia. *Front Pharmacol*. 2018;9:549. doi:10.3389/fphar.2018.00549
55. Surendra BS, Bs S, C M, et al. Bio-mediated synthesis of ZnO nanoparticles using Lantana Camara flower extract: its characterizations, photocatalytic, electrochemical and anti-inflammatory applications. *Environ Nanotechnol Monit Manage*. 2021;15:100442. doi:10.1016/j.enmm.2021.100442
56. Eaton P, Quaresma P, Soares C, et al. A direct comparison of experimental methods to measure dimensions of synthetic nanoparticles. *Ultramicroscopy*. 2017;182:179–190. doi:10.1016/j.ultramic.2017.07.001
57. Tiwari AK, Jha S, Singh AK, et al. Innovative investigation of zinc oxide nanoparticles used in dentistry. *Crystals*. 2022;12(8):1063. doi:10.3390/cryst12081063
58. Enechi OC, Okeke ES, Nwankwo NE, et al. Membrane stabilization, albumin denaturation, protease inhibition, and antioxidant activity as possible mechanisms for the anti-inflammatory effects of flavonoid-rich extract of Peltophorum pterocarpum (DC.) K. Heyne (FREPP) Stem Bark: doi. org/10.26538/tjnpr/v4i10. 25. *Tropical J Nat Prod Res*. 2020;4(10):812–816.
59. Rehman H, Ali W, Zaman Khan N, et al. Delphinium uncinatum mediated biosynthesis of zinc oxide nanoparticles and in-vitro evaluation of their antioxidant, cytotoxic, antimicrobial, anti-diabetic, anti-inflammatory, and anti-aging activities. *Saudi J Biol Sci*. 2023;30(1):103485. doi:10.1016/j.sjbs.2022.103485
60. Manasa DJ, Chandrashekar KR, Pavan Kumar MA, et al. Proficient synthesis of zinc oxide nanoparticles from Tabernaemontana heyneana Wall. via green combustion method: antioxidant, anti-inflammatory, antidiabetic, anticancer and photocatalytic activities. *Results Chem*. 2021;3:100178. doi:10.1016/j.rechem.2021.100178
61. Varghese RM, Kumar A, Shanmugam R. Comparative anti-inflammatory activity of silver and zinc oxide nanoparticles synthesized using Ocimum tenuiflorum and Ocimum gratissimum herbal formulations. *Cureus*. 2024;16(1). doi:10.7759/cureus.52995
62. Nandhini J, Karthikeyan E, Sheela M, et al. Optimization of microwave-assisted green synthesis of zinc oxide nanoparticles using Ocimum americanum and Euphorbia hirta extracts: in vitro evaluation of antioxidant, anti-inflammatory, antibacterial, cytotoxicity, and wound healing properties. *Intelligent Pharm*. 2025;3(1):90–109. doi:10.1016/j.ipha.2024.09.003
63. Mirke NB, Shelke PS, Malavdkar PR, Jagtap PN. In vitro protein denaturation inhibition assay of Eucalyptus globulus and Glycine max for potential anti-inflammatory activity. *Innovations Pharmaceut Pharmacother*. 2020;8(2):28. doi:10.31690/ipp.2020.v08i02.003
64. Elisha IL, Dzoyem J-P, McGaw LJ, et al. The anti-arthritic, anti-inflammatory, antioxidant activity and relationships with total phenolics and total flavonoids of nine South African plants used traditionally to treat arthritis. *BMC Complementary Alternative Med*. 2016;16:1–10. doi:10.1186/s12906-016-1301-z
65. Malaiappan, Priyangha SPT, Niveditha S. Green synthesis and characterization of zinc oxide nanoparticles using Catharanthus roseus extract: a novel approach. *Cureus*. 2024;16(5). doi:10.7759/cureus.60407
66. Dhivyadharshini J, Malaiappan S, Rajeshkumar S. Evaluation of anti-inflammatory and antioxidant activity of Adhatoda vasica zinc nanoparticles. 2021;5950–5964.
67. Yadav E, Yadav P, Verma A. Amelioration of full thickness dermal wounds by topical application of biofabricated zinc oxide and iron oxide nano-ointment in albino Wistar rats. *J Drug Delivery Sci Technol*. 2021;66:102833. doi:10.1016/j.jddst.2021.102833
68. Sheferov I, Balakireva A, Panteleev D, et al. The effect of zinc oxide nanoparticles on properties and burn wound healing activity of thixotropic xymedone gels. *Scientia Pharmaceutica*. 2022;90(4):61. doi:10.3390/scipharm90040061
69. Semis HS, Gur C, Ileriturk M, et al. Investigation of the anti-inflammatory effects of caffeic acid phenethyl ester in a model of λ-Carrageenan–induced paw edema in rats. *Hum Exp Toxicol*. 2021;40(12_suppl):S721–S738. doi:10.1177/09603271211054436
70. Amdekar S, Roy P, Singh V, et al. Anti-Inflammatory Activity of Lactobacillus on Carrageenan-Induced Paw Edema in Male Wistar Rats. Int J Inf. 2012;2012(1):752015. doi:10.1155/2012/752015
71. Meva E, Francois, Essama DM, et al. Anti-inflammatory assessment of zinc oxide nanoparticles mediated Aframomum citratum (C. Pereira) K. Schum (Zingiberaceae) in Wistar rats. *bioRxiv*. 2024. doi:10.1101/2024.12.15.628600.
72. Ovais M, Khalil AT, Raza A, et al. Multifunctional theranostic applications of biocompatible green-synthesized colloidal nanoparticles. *Appl Microbiol Biotechnol*. 2018;102:4393–4408. doi:10.1007/s00253-018-8928-2

73. Moldovan B, David L, Achim M, et al. A green approach to phytomediated synthesis of silver nanoparticles using Sambucus nigra L. fruits extract and their antioxidant activity. *J Mol Liq*. 2016;221:271–278. doi:10.1016/j.molliq.2016.06.003
74. Hmidani A, Hmidani A, Bourkhis B, et al. Phenolic profile and anti-inflammatory activity of four Moroccan date (Phoenix dactylifera L.) seed varieties. *Heliyon*. 2020;6(2). doi:10.1016/j.heliyon.2020.e03436
75. Nunomura W. C-reactive protein (CRP) in animals: its chemical properties and biological functions. *in vitro*. 1992;18:21.
76. Vazquez E, Navarro M, Salazar Y, et al. Systemic changes following carrageenan-induced paw inflammation in rats. *Inflammation Res*. 2015;64:333–342. doi:10.1007/s00011-015-0814-0
77. Jayasri A, Prasad PE, Kumar BD, et al. Antimicrobial and anti-inflammatory activity of Thespesia populnea mediated nanoparticles in murine mastitis model. *Indian J Res Animal*. 2023;57:714–721. doi:10.18805/IJAR.B-5083
78. Yadav E, Singh D, Yadav P, et al. Ameliorative effect of biofabricated ZnO nanoparticles of Trianthema portulacastrum Linn. on dermal wounds via removal of oxidative stress and inflammation. RSC Adv. 2018;8(38):21621–21635. doi:10.1039/C8RA03500H
79. Ihedioha JI, Okafor C, Ihedioha TE. The haematological profile of the Sprague-Dawley outbred albino rat in Nsukka, Nigeria. *Animal Res Int*. 2004;125–132. doi:10.4314/ari.v1i2.40755
80. Oladejo BO, Adiji PI. Effects of lactic acid bacteria on the haematological indices of carrageenan-induced acute inflammation in Wistar Rats. *FUTA J Life Sci*. 2021;1(1):61–70.
81. Kleemann R, Verschuren L, Morrison M, et al. Anti-inflammatory, anti-proliferative and anti-atherosclerotic effects of quercetin in human in vitro and in vivo models. *Atherosclerosis*. 2011;218(1):44–52. doi:10.1016/j.atherosclerosis.2011.04.023
82. Lousinian S, Missopolinou D, Panayiotou C. Fibrinogen adsorption on zinc oxide nanoparticles: a micro-differential scanning calorimetry analysis. *J Colloid Interface Sci*. 2013;395:294–299. doi:10.1016/j.jcis.2013.01.007
83. Sambandam B, Mohan D, Kaliyaperumal P, Raman P, Thiyagarajan D. Acute dermal toxicity of coal fly ash nanoparticles in vivo. *Int J Pharm Pharm Sci*. 2015;2015:403–407.
84. Halarnekar D, Ayyanar M, Gangapriya P, et al. Eco synthesized chitosan/zinc oxide nanocomposites as the next generation of nano-delivery for antibacterial, antioxidant, antidiabetic potential, and chronic wound repair. *Int J Biol Macromol*. 2023;242:124764. doi:10.1016/j.ijbiomac.2023.124764
85. Gajbhiye S, Sakharwade S. Safety Evaluation Of Silver Nanoparticles For Dermal Application. 2021. doi:10.20959/wjpr20217-20780
86. Ezealisiji KM, Siwe-Noundou X, Maduelosi B, et al. Green synthesis of zinc oxide nanoparticles using Solanum torvum (L) leaf extract and evaluation of the toxicological profile of the ZnO nanoparticles–hydrogel composite in Wistar albino rats. *Int Nano Lett*. 2019;9:99–107. doi:10.1007/s40089-018-0263-1
87. Drummer S, Madzimbamuto T, Chowdhury M. Green synthesis of transition-metal nanoparticles and their oxides: a review. *Materials*. 2021;14(11):2700. doi:10.3390/ma14112700

International Journal of Nanomedicine

Dovepress
Taylor & Francis Group

Publish your work in this journal

The International Journal of Nanomedicine is an international, peer-reviewed journal focusing on the application of nanotechnology in diagnostics, therapeutics, and drug delivery systems throughout the biomedical field. This journal is indexed on PubMed Central, MedLine, CAS, SciSearch®, Current Contents®/Clinical Medicine, Journal Citation Reports/Science Edition, EMBase, Scopus and the Elsevier Bibliographic databases. The manuscript management system is completely online and includes a very quick and fair peer-review system, which is all easy to use. Visit http://www.dovepress.com/testimonials.php to read real quotes from published authors.

Submit your manuscript here: https://www.dovepress.com/international-journal-of-nanomedicine-journal